PLOS ONE

Spatial ecology of moose in Sweden: Combined Sr-O-C isotope analyses of bone and antler

Elena Armaroli [1]*, Federico Lugli [1,2,3]*, Anna Cipriani [1,4], Thomas Tütken [5]

1 Department of Chemical and Geological Sciences, University of Modena and Reggio Emilia, Modena, Italy, 2 Institut für Geowissenschaften, Goethe Universität Frankfurt, Frankfurt am Main, Germany, 3 Department of Cultural Heritage, University of Bologna, Ravenna, Italy, 4 Lamont-Doherty Earth Observatory, Columbia University, Palisades, NY, United States of America, 5 Arbeitsgruppe für Angewandte und Analytische Paläontologie, Institut für Geowissenschaften, Johannes Gutenberg–Universität Mainz, Mainz, Germany

* elena.armaroli@unimore.it (EA); lugli@em.uni-frankfurt.de (FL)

Abstract

The study of spatial (paleo)ecology in mammals is critical to understand how animals adapt to and exploit their environment. In this work we analysed the $^{87}Sr/^{86}Sr$, $\delta^{18}O$ and $\delta^{13}C$ isotope composition of 65 moose bone and antler samples from Sweden from wild-shot individuals dated between 1800 and 1994 to study moose mobility and feeding behaviour for (paleo)ecological applications. Sr data were compared with isoscapes of the Scandinavian region, built *ad-hoc* during this study, to understand how moose utilise the landscape in Northern Europe. The $^{87}Sr/^{86}Sr$ isoscape was developed using a machine-learning approach with external geo-environmental predictors and literature data. Similarly, a $\delta^{18}O$ isoscape, obtained from average annual precipitation $\delta^{18}O$ values, was employed to highlight differences in the isotope composition of the local environment vs. bone/antler. Overall, 82% of the moose samples were compatible with the likely local isotope composition (n = 53), suggesting that they were shot not far from their year-round dwelling area. 'Local' samples were used to calibrate the two isoscapes, to improve the prediction of provenance for the presumably 'non-local' individuals. For the latter (n = 12, of which two are antlers and ten are bones), the probability of geographic origin was estimated using a Bayesian approach by combining the two isoscapes. Interestingly, two of these samples (one antler and one bone) seem to come from areas more than 250 km away from the place where the animals were hunted, indicating a possible remarkable intra-annual mobility. Finally, the $\delta^{13}C$ data were compared with the forest cover of Sweden and ultimately used to understand the dietary preference of moose. We interpreted a difference in $\delta^{13}C$ values of antlers (^{13}C-enriched) and bones (^{13}C-depleted) as a joint effect of seasonal variations in moose diet and, possibly, physiological stresses during winter-time, i.e., increased consumption of endogenous ^{13}C-depleted lipids.

---

1. Introduction

The study of species dynamics through space and time, including their movements, feeding behaviour, interactions and responses to environmental and anthropogenic factors, constitutes the complex field of spatial ecology [1, 2]. This discipline is increasingly applied to conservation and management issues to find effective ways to preserve biodiversity in an era of profound environmental change [3–6]. In fact, the changing climate and its consequences (e.g., droughts, wildfires, floods, hurricanes), further accelerated by human activities, are causing disturbance of natural habitats in increasingly unpredictable ways. Therefore, it has become important to understand how species respond to our changing world and implement ways to protect our biodiversity [7, 8].

The first step in enabling biodiversity and ecosystem preservation is to study how wildlife species move across the landscape and to quantify and predict their spatial distribution [9, 10]. Today this is possible through an integrative approach that brings together ecological theory and statistical modelling [11–14]. At the same time, to interpret present and future environmental changes it is important to understand what changes have occurred over time. This requires more multidisciplinary research, enabling collaboration among archaeologists, historians, and natural scientists [15–17].

Animal movements are commonly reconstructed by satellite imaging/GPS tracking [18], yet this approach requires marking or recapturing individuals, precluding retrospective investigations from sampled tissues and from archaeological/paleontological specimens. In this sense, biogeochemical markers can help unravel animal life-histories and migratory behaviour. Indeed, geochemistry has long been used for provenance and environmental studies, with applications ranging from food science to ecology, forensics and archaeology [19–23]. It is now well established that mobility and nutritional patterns are recorded in the geochemical signature of human and animal skeletal tissues [24–26]. To date, numerous applications of strontium ($^{87}Sr/^{86}Sr$), oxygen ($\delta^{18}O$) and carbon ($\delta^{13}C$) isotope analyses have reconstructed dietary habits, migration events, residential patterns, animal management, exchange of goods and raw materials in archaeological contexts [27–30].

Studies on modern animals' spatial ecology are key in understanding how isotopes are linked with individual mobility. This is due to the fact that modern animal behaviour is known and can be compared with findings obtained through geochemical analyses [31]. Moreover, modern samples are not affected by diagenetic modification of bone bioapatite, avoiding the problems of obtaining pristine isotopic compositions [32, 33]. Altogether, modern tissues are thus ideal control samples for calibrating our inferences about past mobility from fossil specimens [34, 35].

A key aspect in provenance studies that use isotope analyses, is the determination of bioavailable Sr in the area of interest to determine whether the individual or object under investigation is local or not [36, 37]. However, this is not sufficient to determine where they came from. In recent years much attention has been focused on the construction of both local and global isoscapes (i.e. isotope distribution maps) to enable the prediction of the place of origin of unknown samples using both Sr and O isotope data [38–40].

Here we used modern and historical *Alces alces* (Linnaeus, 1758) samples (time range 1800–1994) from Sweden to understand the potential of isotope markers in unraveling moose home-range and migratory behaviour. To this end, we measured Sr, O and C in moose bones and antlers and compared their values with a novel built isoscape of the Scandinavian region.

Moose is the largest member of the Cervidae family, distributed in the circumpolar boreal forests of Eurasia and North America [41, 42]. The size of moose populations and their distribution in Europe has changed over time [43–45]. Today moose are widely distributed in

Scandinavia and are the dominant large herbivore in Sweden. This animal is currently the focus of an increasing amount of research on its management and conservation [46, 47]. Monitoring moose behaviour has proven to be crucial in finding an effective way to control their population density and detect the effect of their browsing activity on forest damage (including damage to economically important tree species in the region) [48–51]. The importance of moose browsing and the need to integrate it into management practices were also recently highlighted by Salisbury *et al.* [52]. They demonstrated the role of moose browsing activity in shaping landscape structure and boreal forest composition, with a net impact on climate [52]. Overall, monitoring and predicting moose movements in the landscape are essential for planning both moose and forest management practices, especially in relation to the growing concern about the effects of climate change on animal migration and biodiversity conservation [15, 53–55].

Since both migrant and non-migrant individuals are often present within the same population [56, 57], much attention has been focused on understanding their movement behaviour, often using the GPS tracking system. For example, some researchers have studied the interaction between wolves (predator) and moose (prey) [58, 59]. Others have attempted to detect differences in the moose home-range and behaviour in relation to age and sex [54, 60], season [54, 61], snow quality and depth [56, 62], foraging strategies [63] and habitat deterioration [64, 65].

Most research on moose has focused on a single population living in a restricted area of Scandinavia (but see [47]). Here we present a large amount of samples distributed throughout Sweden. This represents a rare opportunity to study the mobility of a large herbivore such as moose on a large scale. To date, isotopic analyses on moose samples have been conducted for ecological studies focused on diet, using mainly N (δ^{15}N) and C (δ^{13}C) stable isotopes [66–70]. To our knowledge, this is the first time that Sr and O isotopes are used together to analyse moose large-scale mobility in Sweden. Furthermore, no one has yet attempted to build a complete multi-proxy Sr isoscape of Scandinavia, here developed through a machine-learning model and literature data. In fact, although much attention has been focused on Sr isotope analysis for past mobility studies in Scandinavia (see among others [71–77]), today only baselines of constrained areas (i.e., mainly those characterised by archaeological discoveries) are available [78–80].

The Sr, C, and O isotope analyses on modern moose samples will be useful as an integrative approach to modern ecological studies on this animal. They will complement traditional methods of tracking mobility (e.g., radio-, satellite- and GPS-tracking) as well as genetic analyses [81, 82], providing a new tool for management and conservation practices. The methodology used here can also be applied to areas other than Scandinavia and to animals other than moose, becoming a useful tool for global biodiversity conservation in the current period of environmental change. Moreover, this approach could be transferred to the study of faunal and human mobility in the past, implementing the growing research field of geostatistics applied to archaeological research (see e.g., [83]).

2. Isotopes for tracing mobility and diet

Strontium is an alkaline earth element with four naturally occurring isotopes: ^{84}Sr ($\sim 0.56\%$), ^{86}Sr ($\sim 9.87\%$), ^{87}Sr ($\sim 7.04\%$) and ^{88}Sr ($\sim 82.53\%$). All but ^{87}Sr are stable, while this latter is radiogenic, forming by the β-decay of ^{87}Rb with a half-life of 4.88×10^{10} years. Strontium becomes incorporated into the local ecosystem through bedrock weathering, being transferred to soil, where it mixes with groundwaters, surface waters and atmospheric depositions. Sr is then transported to the oceans mainly from rivers as dissolved ions in water or through transport of sediments. Bioavailable Sr is taken up by vegetation through the root uptake and by animals through food and drinking water, with limited fractionation; moreover, any eventual isotope

effect is corrected after mass bias normalization to an internal stable isotope ratio (i.e. $^{88}Sr/^{86}Sr$ or $^{86}Sr/^{88}Sr$) [84–87]. Sr substitutes then for calcium in the hydroxylapatite [$Ca_{10}(PO_4)_6OH_2$] of vertebrate skeletal tissues. Taken together these characteristics make $^{87}Sr/^{86}Sr$ a powerful tool to trace geographically biological [88] and environmental materials [85, 89].

Oxygen has three naturally occurring stable isotopes: ^{16}O (99.757%), ^{17}O (0.038%), ^{18}O (0.205%). Because of their higher abundance, the ratio between the heavy isotope ^{18}O to the light isotope ^{16}O of a particular material ($\delta^{18}O$) is commonly determined in geochemistry [90, 91]. The oxygen in mammalian body water comes mainly from drinking water, but also from oxygen structurally bound to organic compounds in food and atmospheric O_2 inhaled by respiration [92–94]. The $\delta^{18}O$ (and its fractionation) of these sources is affected by multiple factors (e.g., precipitation, temperature, humidity, continentality, altitude, latitude), which differ from one geographical area to the other [26, 38]. The $\delta^{18}O$ has thus become key in provenance studies in archaeology, used for example in the study of seasonal vertical transhumance [95] and paleoenvironmental reconstruction [96], often in combination with other isotope systems [97].

Carbon has two stable isotopes, ^{12}C (98.93%) and ^{13}C (1.07%). ^{13}C has a mass 8.36% greater than that of ^{12}C, causing the C isotopes to fractionate in chemical and biological processes [91, 98]. The $\delta^{13}C$ value of plant tissues mainly changes depending on the CO_2 fixation process used [99,100], allowing the distinction between C_3 and C_4 plants [101]. In addition, the $\delta^{13}C$ value can be influenced by the so called "canopy effect", which causes a depletion of the $\delta^{13}C$ of forest plants due to a number of factors including reduced light levels and re-assimilation of ^{13}C-depleted CO_2 [102, 103]. The $\delta^{13}C$ is widely used in archaeological research both for dietary and paleoenvironmental reconstruction [101, 104], but also for the study of animal management and faunal migration in combination with $\delta^{18}O$ and $^{87}Sr/^{86}Sr$ values [105, 106].

3. Materials and methods

3.1 Study area

Scandinavia, known as the Scandinavian Peninsula, is a region in Northern Europe characterised by diverse lithologies and a complex geological history, which has shaped this landscape since the Archean. The bedrock is composed of three primary components categorised based on the timing of rock crystallisation, deposition, and crustal growth: 1) Precambrian crystalline rocks forming the Baltic Shield also known as the Fennoscandian Shield, 2) the so-called Caledonides, rocks of the Caledonian orogeny (0.5–0.4 giga-annum; Ga), and 3) Phanerozoic to Neoproterozoic sedimentary rocks [107].

The Precambrian basement, primarily composed of granites, gneisses and greenstone belts forms the core of the Scandinavian Peninsula. It is exposed in large areas of Norway, Sweden and Finland. The oldest rocks, dated between 2500 and 3100 mega-annum (Ma), are found in the northeast portion of the Fennoscandian Shield, in the Kola Peninsula, Karelia and northeastern Finland. Archean rocks of 2600 to 2800 Ma also outcrop in the northernmost part of Sweden. Metasedimentary and metavolcanic rocks, as well as multiple generations of granitoids, hosting important ore deposits, dated between 1750 and 1900 Ma, formed during the Svecofennian orogeny and outcrop mainly in northern and central Sweden as well as in the southwestern part of Finland. Part of the Baltic Shield is also the Transscandinanavian igneous belt (TIB), consisting of largely undeformed granitoids and associated porphyries, emplaced between 1850 and 1650 Ma. This is a $\sim$ 1400 km long belt running across the Scandinavian Peninsula, from Småland in southern Sweden through Värmland and western Dalarna and continuing under much of the Caledonian nappes up to northern Scandinavia, cropping out in small tectonic windows [108, 109].

The Caledonides were formed during the collisional event between the continents of Baltica and Laurentia around 450–400 Ma ago, and stretch through most of Norway and in the mountainous northwestern part of Sweden. Sedimentary and volcanic rocks were deposited in the Iapetus Ocean, between the late Proterozoic and Silurian periods, 700 to 400 Ma ago, and during the Caledonian orogeny were thrusted eastwards over the Fennoscandian Shield together with slices of the crystalline basement. The Caledonian rocks consist of high-grade metamorphic rocks and (meta)sedimentary rocks also partially intruded by magmatic rocks [110, 111].

Sedimentary rocks from the Phanerozoic, less than 545 Ma, are found on top of the Precambrian shield region. Sandstones, shales and limestones dated between 540 and 420 Ma ago outcrop across extensive areas in southern Sweden, including the islands of Öland and Gotland. Mesozoic and Tertiary sediments (younger than 250 Ma) are found in southernmost Sweden (Skåne) and in Denmark [112].

A relatively small outcrop of Permian magmatic rocks ca, 250 Ma old forms the Oslo Graben, a failed rift system created during the Variscan orogeny [113].

3.2 Sample collection and description

Moose bone and antler specimens of adult individuals were sampled in the zoological collection of the Naturhistoriska Riksmuseet in Stockholm, Sweden. No permits were required for the described study, which complied with all relevant regulations. About 50–100 mg powder of bone or antler were drilled manually using a handheld Proxxon drill with diamond studded drill bits. Samples were mostly taken from crania (n = 50) and some from antlers (n = 15), collected covering different bedrock types across Sweden (Fig 1). Antlers were sampled in a cm-size area close to the base (lower part of the antler), representing an estimated period of life less than one month during spring. Overall, n = 29 samples are males, n = 17 females, and n = 19 of unknown sex. Details about the sampled specimens such as sample ID, geographic location, year of death are provided in S1 Table. Bones and antlers have different formation times (i.e., several years and a few months, respectively; see below). For this reason, we have interpreted and discussed the results separately. In addition, we acknowledge that because we are dealing with bone and antler samples from different individuals, our interpretation concerns general aspects of moose ecology, rather than individual-level inferences.

The spatial distribution of the analysed moose samples is reported in Fig 1 and plotted over a geological map of Scandinavia. Latitude and longitude values for each sample are reported in S1 Table.

3.3 Isotope analyses

Strontium ($^{87}Sr/^{86}Sr$), oxygen ($\delta^{18}O$) and carbon ($\delta^{13}C$) were measured on a total of 65 bone and antler samples of modern and historical wild-shot *Alces alces* from Sweden. The O and C isotopes were measured on the carbonate portion of the skeletal tissues by using a Gasbench II coupled to a Delta Plus XL IRMS at the University of Tübingen (Tübingen, Germany). Prior to isotope analysis 10 mg of bone powder was pretreated with 2M NaOCl and 0.1 M acetic acid according to the protocol of Koch *et al.* [115] in order to remove organic matter [116]. About 2 mg of pretreated bone powder was reacted for 90 mins at 70˚C with phosphoric acid and normalised to a calibrated Laaser marble standard. As quality controls two international carbonate reference materials were measured yielding values in line with certified oxygen and carbon isotope compositions (NBS 18 $\delta^{18}O_{VPDB}$ = -23.13±0.09‰, $\delta^{13}C_{VPDB}$ = -4.97±0.04‰, n = 3; NBS 19: $\delta^{18}O_{VPDB}$ = -2.22±0.12‰ and $\delta^{13}C_{VPDB}$ = +1.93±0.10‰, n = 3). VPDB values were converted to $\delta^{18}O_{VSMOW}$. Carbonate $\delta^{18}O$ values were converted in phosphate ($\delta^{18}O_{PO4}$) ([117]; all mammals; $\delta^{18}O_c$ = 1.037*$\delta^{18}O_{PO4}$ + 8.57) and then in $\delta^{18}O$ of ingested water
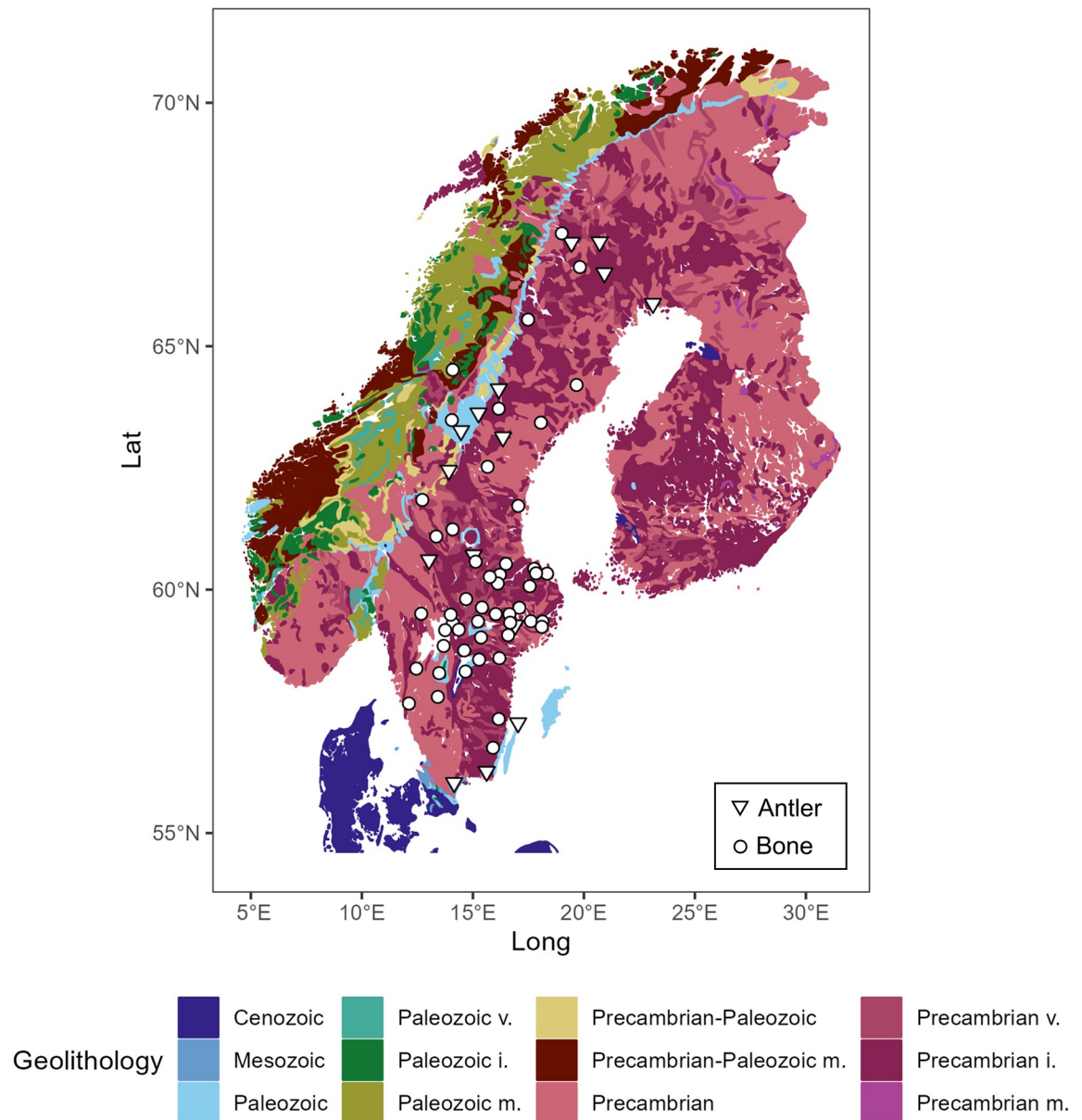
Fig 1. Samples distribution across Sweden. Moose bones (white dots) and antlers (white triangles) are plotted over the geolithological map of Scandinavia. Main stratigraphic units by age are reported; type of lithology is indicated when explicitly reported in the USGS source file: v = volcanic, i = intrusive, m = metamorphic. The map is based on the European geo4_2l shapefile from USGS [114].

https://doi.org/10.1371/journal.pone.0300867.g001

($\delta^{18}O_w$) by using the formula for deer of D'Angela and Longinelli [118]. Given the lack of species-specific conversion-equations for moose, the deer equation of [118] represents a close approximation in terms of taxonomy (*Cervidae*) and dietary behaviour (both ruminant herbivores). Carbon isotope values were corrected for anthropogenically induced variation of CO_2 $\delta^{13}C$ and reported to a 1994 year-value, by following the workflow of Long *et al*. [119], but using a LOESS model to fit the data of Francey *et al*. [120]. The $\delta^{13}C$ data reported to a 1800 year-value are also listed in S1 Table. Sr isotopes were measured at the Geochemistry Lab of the Department of Chemical and Geological Sciences (University of Modena and Reggio Emilia; https://www.geochem.unimore.it/). About 5 mg of bioapatite powder for each sample was

dissolved in 3M HNO_3. The Sr separation from the matrix was performed through chromatographic Teflon columns filled with 30 μl of Eichrom Sr spec resin [121, 122]. Once the columns were cleaned with MilliQ, the dissolved samples were loaded and the cations (not Sr) were desorbed by percolating 3M HNO_3, to eliminate matrix ions. Strontium was then eluted using MilliQ. The Sr samples were diluted with 4% HNO_3 at 50 ppb and analysed with a Neptune MC-ICPMS at Centro Interdipartimentale Grandi Strumenti of the University of Modena and Reggio Emilia. ^{82}Kr, ^{83}Kr, ^{84}Sr, ^{85}Rb, ^{86}Sr, ^{87}Sr and ^{88}Sr m/z were collected with 10^{11} and 10^{12} (for ^{82}Kr, ^{83}Kr and ^{84}Sr) Ω resistors. Background subtraction and Rb correction was performed with routine methods (see [123]); similarly, mass bias normalisation used an exponential law and an ^{88}Sr/^{86}Sr ratio of 8.375209 [124]. Samples' ^{87}Sr/^{86}Sr ratios were reported to an accepted NIST-SRM 987 value of 0.710248. Repeated analyses of the NIST-SRM 987 yielded an average ^{87}Sr/^{86}Sr ratio of 0.710228 ± 0.000018 (2 SD, n = 20).

3.4 Geostatistical framework

Several studies have been conducted to determine which materials are most suitable for establishing the local Sr baseline and building the isoscapes [125]. Today there is general agreement on the preferential use of archaeological microfauna, snails, modern plant and water samples [36, 37, 126, 127]. Other natural materials useful for provenance studies include soil leachates [128] as well as modern and archaeological faunal tooth enamel and bones, provided they are local to the area under study and free of any contamination or diagenetic modification [36, 129].

Given these assumptions, the first step in building the Sr isoscape was to collect bibliographical data of natural samples' ^{87}Sr/^{86}Sr, including vegetation, waters, soil leachates, snails, animal bones and teeth (both modern and archaeological) from Sweden and surrounding countries (i.e., Norway, Finland and Denmark; see S2 Table). Only local fauna (as described in the respective paper) was selected, including snails, microfauna, animals with a small home-range, and domestic animals. Among the natural samples, we preferably selected plants and waters as the more representative of the local bioavailable Sr pool. Soil leachates were added only if no other type of sample was available for a given site. Moreover, since as pointed out earlier the ^{87}Sr/^{86}Sr values are only available for limited areas of Scandinavia, we added the ^{87}Sr/^{86}Sr values of modern soil leachates from GEMAS project [128] to our database to cover as many territories as possible. All the further data analyses were carried out in R (version 4.0.5).

To build the Sr isoscape map of Scandinavia we used Random Forest regression (RF) with multiple predictors (*randomForest* package; [130]), following the method of Bataille *et al.* [40]. The Random Forest is a supervised tree-based machine learning algorithm that uses a labelled database including environmental and geological information to predict the isotope ratios in areas with similar features [39, 40, 131]. Seven external variables, obtained from global raster maps (see [40]), were selected by *VSURF* [132] based on their importance in predicting the ^{87}Sr/^{86}Sr ratio. After the map outline, a 10-fold cross-validation was performed to estimate the power of the prediction, evaluated as RMSE (Root mean square error). To generate a spatial-uncertainty map, we employed a quantile RF regression (*ranger* package; [133]), then halving the RF $q_{0.84}$ - $q_{0.16}$ difference (i.e., lower and upper limits of a ∼68% interval; [134]). The Sr isoscape and the error map can be found as S1 and S2 Files, respectively. To test the Sr natural variability vs. the RF error, we gathered all the data with the same coordinates from S2 Table and calculated the ^{87}Sr/^{86}Sr standard deviations (SD) from each site. As depicted in S1 Fig, both the observed SDs (S1A Fig; R^2 = 0.46, p < 0.01) and the calculated RF error from the error map (S1B Fig; R^2 = 0.74, p < 0.01) are correlated with the mean ^{87}Sr/^{86}Sr of the site. This suggests that both errors and isotope variability are higher in high-radiogenic areas, as

expected (see e.g., [39, 131]). The observed SD among the samples and the calculated RF error from the error map are also correlated with each other (S1C Fig; $R^2 = 0.36$, $p < 0.01$), with an average difference of 0.0024 ± 0.0043. The RF error tends to underestimate the observed local isotopic variability at sites with elevated $^{87}Sr/^{86}Sr$ ratios (S1C Fig).

The oxygen isoscape (annual average value) was downloaded from *waterisotopes.org* and cropped for the area of interest. This represents the mean modelled climatological prediction based on annual precipitations [20]. A conservative 1‰ constant spatial uncertainty was arbitrarily associated with each pixel of the oxygen isoscape. This error is 10-times larger than the median error associated with the model (~ 0.1‰) and compatible with the spatial uncertainty used in other works (e.g., [135–137]).

To assess the 'local vs non-local' isotope signature, we checked the difference between the isotope ratio of the samples themselves and the isoscapes at their position ($\Delta^{87}Sr/^{86}Sr_{sample\text{-}isoscape}$ and $\Delta^{18}O_{sample\text{-}isoscape}$). To do so, we extracted and averaged pixel values from the maps at sample location, with a buffer radius of 10 km. The buffer value to be used was chosen, testing different radius lengths (from 1 km to 250 km) and selecting the resulting linear model (ordinary least square of sample vs. isoscape isotope ratios) with the highest coefficient of determination (see S3 Table) and compatible with expected moose home ranges from ecological data (see Discussion). Samples within 1 standard-deviation (1σ thereafter) of the $\Delta^{87}Sr/^{86}Sr_{sample\text{-}isoscape}$ and $\Delta^{18}O_{sample\text{-}isoscape}$ distributions were thus considered as compatible with the local area (10 km radius buffer), also accounting for the isoscape(s) spatial uncertainty (see Results). Both the isoscapes were then calibrated using a linear fit with the moose samples within 1σ (i.e., those likely 'local'); values outside 1σ-variability of either $\Delta^{87}Sr/^{86}Sr_{sample\text{-}isoscape}$ or $\Delta^{18}O_{sample\text{-}isoscape}$ were thus removed from the calibration.

Samples outside 1σ-variability of the isoscape Δs, thus likely different from the local-buffer area, were compared with the isoscapes using a Bayesian probabilistic approach and the '*assignR*' package in R [138]. The prior probability assumes that all grid cells are equally likely locations of origin of these samples. The posterior probability of origin is computed at each grid cell, returning a raster object which contains one probability density surface per sample with its likely provenance. In the calculations, raster maps with prediction errors of the modelled isoscapes are also included. The Sr and O obtained posterior probabilities were joint to obtain a final combined dual-estimation.

To test the effect of forest cover on $\delta^{13}C$ of moose samples, pixels of a Sweden forest cover map (from [139]; time span 0–125 years BP) were extracted with a 10-km buffer radius at the (moose) sample locations. The forest cover maps of [139] are based on remote-sensing data, calibrated through (fossil) pollen records and represent a full range of pixel values from 0 to ~ 90% canopy closure. Then, ordinary least square models of sample $\delta^{13}C$ tissues vs. %-forest cover were calculated; 'non-local' moose based on Sr-O were excluded.

The R code is available online on Zenodo: https://zenodo.org/records/10418660.

4. Results

The complete list of isotopic results, along with all the information about the samples, are available in S1 Table. Strontium, oxygen and carbon data are shown in Fig 2(A)–2(E). Since bone and antler represent different time averages (i.e., several years and a few months, respectively) [69, 140] we decided to present bone and antler data separately.

Strontium isotopes ($^{87}Sr/^{86}Sr$) of moose antlers range between 0.71309 and 0.75305 with a mean value of 0.72631 (± 0.01022, 1 SD, n = 15). Bones yielded also a similarly wide range with ratios between 0.71192 and 0.75017 but the mean value is more radiogenic and equals 0.73133
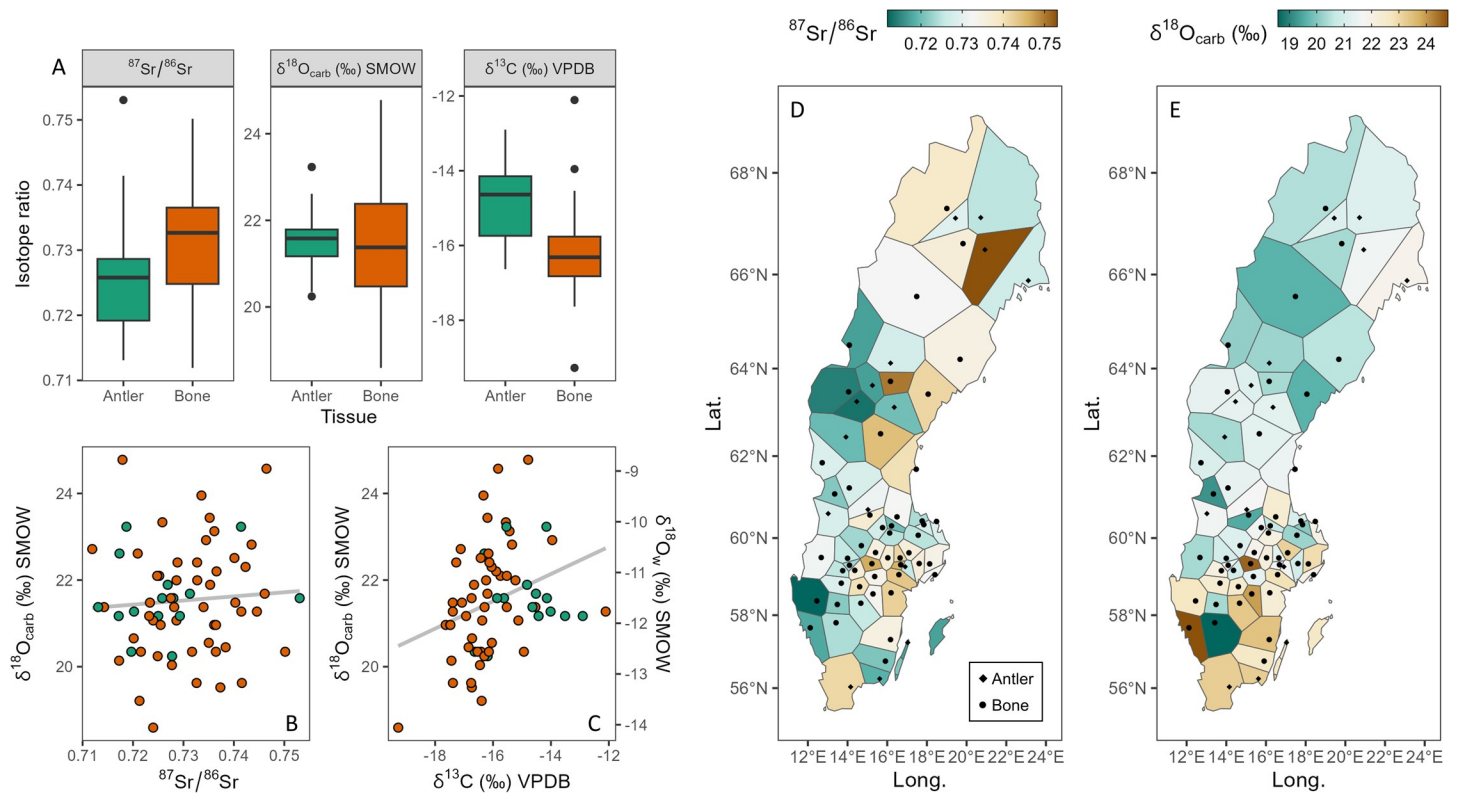
Fig 2. Strontium, oxygen and carbon isotope data of moose antlers and bones. A) Boxplot of strontium, oxygen and carbon isotope data of antlers (green; n = 15) and bones (orange; n = 50). B) $\delta^{18}O$ values of antlers and bones versus their respective $^{87}Sr/^{86}Sr$ and C) $\delta^{13}C$ values; color coding as in (A); grey lines are linear regressions through the data. D) Voronoi diagram of moose's Sr isotope values plotted over the map of Sweden. E) Voronoi diagram of moose's oxygen isotope values plotted over the map of Sweden.

https://doi.org/10.1371/journal.pone.0300867.g002

($\pm$ 0.00887, 1 SD, n = 50). Such radiogenic values clearly reflect the geology of Scandinavia, dominated by old rocks.

Oxygen isotopes ($\delta^{18}O_{SMOW}$) of the carbonate moiety structurally bound in the bioapatite of moose antlers yielded a mean value of +21.6‰ ($\pm$ 0.9, 1 SD, n = 15), ranging between +20.2 and +23.2‰. Similarly, bones yielded a mean $\delta^{18}O$ value of +21.5‰ ($\pm$ 1.3, 1 SD, n = 50), ranging between +18.6 and +24.8‰. Once converted in water values, oxygen isotopes agree with values observed in Scandinavia (see *waterisotopes.org* and Fig 3B).

Carbon isotopes ($\delta^{13}C_{VPDB}$ corrected for CO_2, see Materials and Methods) of the carbonate portion of bioapatite of moose antlers vary between -16.6 and -12.9‰ with a mean value of -14.9‰ ($\pm$ 1.1, 1 SD, n = 15). Bones yielded a wider range between -19.3 and -12.1‰ with a mean of -16.2‰ ($\pm$ 1.1, 1 SD, n = 50). These values are typical of C_3 plants feeders, in agreement with C_3 and C_4 plants distribution in Europe [21, 100, 141]. No statistically significant correlation was found between $\delta^{13}C$ values of moose tissues and forest cover (bone R^2 = 0.001, *p* = 0.801; antler R^2 = 0.03, *p* = 0.52; combined R^2 = 0.02, *p* = 0.22).

We tested the correlation between oxygen and strontium isotopes (Fig 2B; R^2 = 0.005, *p* = 0.570), and the correlation between oxygen and carbon isotopes (Fig 2C; R^2 = 0.098, *p* = 0.011). In both cases there is no significant linear trend.

The Sr isoscape (Fig 3A) obtained through RF with 7 external predictors (*r.srsrq3*, *r.fert*, *r. elevation*, *r.ssa*, *r.cec*, *r.ssaw* and *r.mat*, see [40]) yielded RMSE = 0.0055 and R^2 = 0.65. For additional details about the isoscape see S2 Fig. The modelled isoscape varies between 0.70519
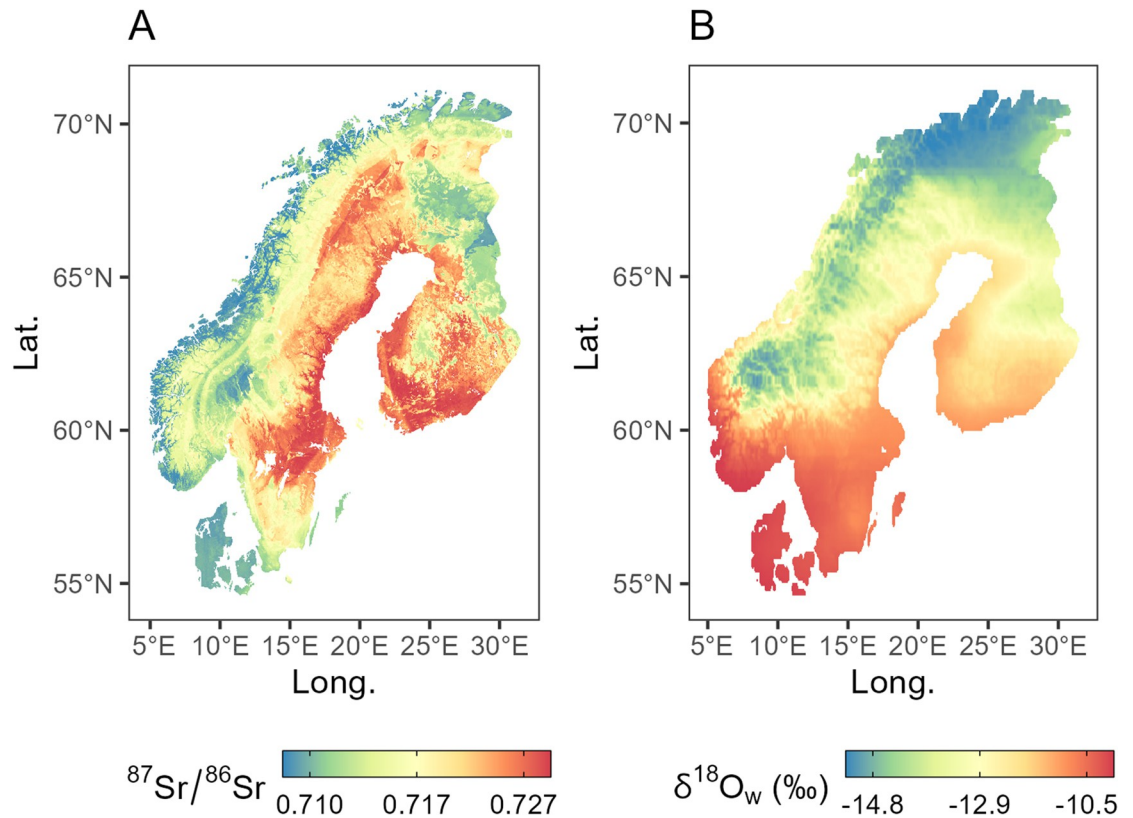
Fig 3. Isoscapes. A) ^{87}Sr/^{86}Sr isoscape built through Random Forest with n = 7 external predictors; B) δ^{18}O isoscape (mean annual precipitation values) downloaded from *waterisotopes.org*. Maps are colored through a quantile scale ($q_{0.1}$, median, $q_{0.9}$); min and max values for the ^{87}Sr/^{86}Sr isoscape (A) are: 0.705 and 0.748, respectively; while for the δ^{18}O isoscape (B) are -17.3 and -7.1‰.

https://doi.org/10.1371/journal.pone.0300867.g003

to 0.74820, with a median of 0.71714. Bataille *et al.* [142]'s model product *r.srsrq3* is the more dominant predictor, indicating that the bedrock geology and rock age impacted the modelled Sr isotope values. The importance of *r.fert* (fertilisation rate) in the prediction is likely due to the fact that GEMAS soils (used in the interpolation) are mainly agricultural soils and thus potentially affected by the use of N- and P-based fertilisers. Sea salt deposition (*r.ssaw* and *r. ssa*) also strongly contributed to the Sr isotope variability observed in the isoscape (see e.g., the relatively low Sr isotope ratios along the Norway coastline). Locally, elevation (*r.elevation*) seems to drive the isoscape ^{87}Sr/^{86}Sr, with low isotope values at mid-low-elevations ($\sim$200 m; see S2 Fig). This is possibly due to the exposure by tectonic and subsequent erosion of deeper portions of the crust with different lithologies (e.g., see gradient from Norway coast to the Caledonides mountain range).

The oxygen isoscape (Fig 3B) varies between -17.3 to -7.1‰, with a median of -12.9‰. As expected, a latitudinal trend is observed, with the most positive values in the south and the most negative values in the north. This trend reflects the typical distribution of oxygen isotopes in precipitation due to the progressive condensation of the vapour during transport to higher latitudes with lower temperatures. Oxygen isotopes tend to be depleted in ^{18}O as elevation increases and this can be seen in profiles from sea level to the mountainous areas of Sweden and Norway.

We calculated the difference between the isotope ratio of the samples and the isoscapes at their position (Fig 4A). The Δ^{87}Sr/^{86}Sr$_{sample-isoscape}$ yielded a median value of 0.0052, ranging

between -0.0094 to 0.0313. The $\Delta^{18}O_{sample-isoscape}$ yielded a median value of 0.3, ranging between -3.9 to 2.1. No spatial trend is evident plotting the delta over the Scandinavia map (S3 Fig). Overall, this suggests that the Sr isoscape slightly underpredicts the moose Sr isotope biological values. This could be related to several factors such as: 1) the GEMAS dataset is composed by soil leachates, which may show $^{87}Sr/^{86}Sr$ shifted to the local carbonate end-member, i.e., less radiogenic values; 2) the isoscape data density is higher in some specific areas (e.g., archaeological sites), and not evenly distributed throughout the region; 3) intrinsic limits of the modelling method itself (see S2 Fig); 4) moose diet is on average more radiogenic than the expected local bioavailable Sr (e.g. ingestion of silica dust; reliance on plants with deep rooting depth); 5) changes in the bioavailable $^{87}Sr/^{86}Sr$ across time due to e.g. the eventual loss of forested areas [143]. On the other hand, the oxygen isotope values of the isoscape seem to better predict the sample oxygen isotope values.

We tried to identify any difference in the $\Delta^{87}Sr/^{86}Sr_{sample-isoscape}$ and $\Delta^{18}O_{sample-isoscape}$ between sexes. We found $p = 0.89$ and 0.04 (non-parametric Mann-Whitney U test), respectively (S4 Fig). This means that the sexual difference in the $\Delta^{87}Sr/^{86}Sr_{sample-isoscape}$ is not statistically significant, while the $\Delta^{18}O_{sample-isoscape}$ sexual difference is significant at $p = 0.05$. Considering bone samples only, the difference is not significant both for the $\Delta^{87}Sr/^{86}Sr_{sample-isoscape}$ and the $\Delta^{18}O_{sample-isoscape}$ values ($p = 0.63$ and $p = 0.77$, respectively), suggesting that the observed significant $\Delta^{18}O_{sample-isoscape}$ sexual difference was driven by the presence of antlers in the dataset. Overall, this indicates that the sex is not a driving factor in the $\Delta_{sample-isoscape}$ values. We indeed found a statistically significant difference in $\Delta^{18}O_{sample-isoscape}$ between antler and bone tissues at $p = 0.05$ (non-parametric Mann-Whitney U test, $p = 0.001$ all sample considered; $p = 0.03$ male only), with median $\Delta^{18}O_{sample-isoscape}$ of antlers higher than bones ($\sim 1‰$). This likely reflects the period of antler growth, namely during warm seasons (spring-summer; [144]), and thus registering relatively higher $\delta^{18}O$ values of ingested water.

Since most of the $\Delta^{87}Sr/^{86}Sr$ values are positive (Fig 4A) and given the good correlation between the samples and the isoscapes (Fig 4B and 4C), we choose to linearly calibrate both the isoscapes using the samples within ± 1σ. After removing the 1σ-outliers, the linear fit between the $^{87}Sr/^{86}Sr_{sample}$ and the $^{87}Sr/^{86}Sr_{isoscape}$ shows an R^2 of 0.35 ($p < 0.01$; intercept = 0.15 ± 0.10; slope = 0.80 ± 0.15), while the linear fit between the $\delta^{18}O_{sample}$ and the $\delta^{18}O_{isoscape}$ shows an R^2 of 0.51 ($p < 0.01$; intercept = -3.4 ± 1.1; slope = 0.70 ± 0.09). The calibrated isoscapes are on average more positive/higher (0.0055 for Sr and 0.50 for oxygen) than the uncalibrated ones (see S5 Fig). Due to the large spatial uncertainties associated with both isoscapes (see Figs 4 and S6), we considered individuals within the 1σ-variability as likely compatible with the local isotope signature, in a buffer-radius of 10 km.

We used the calibrated isoscapes to test the provenance of the 1σ-outliers and their probability distance of origin (Figs 5 and 6). Although in some cases the probability distributions display the highest values at more than 250 km (up to 1000+ km), the most likely distance travelled is perhaps less than 100 km, i.e., compatible areas closest to the place of death, where increases in probability distributions are already evident (see Discussion below). The only samples for which a higher degree of mobility can be assumed confidently are G_EL_113 (antler) and K_EL_127 (bone). In fact, their probability distributions begin to increase at 250 km of distance.

5. Discussion

5.1 Strontium and oxygen isotopes: Moose mobility

In the current period of environmental change, the study of faunal mobility across the landscape has become increasingly important. Quantifying and predicting the spatial distribution
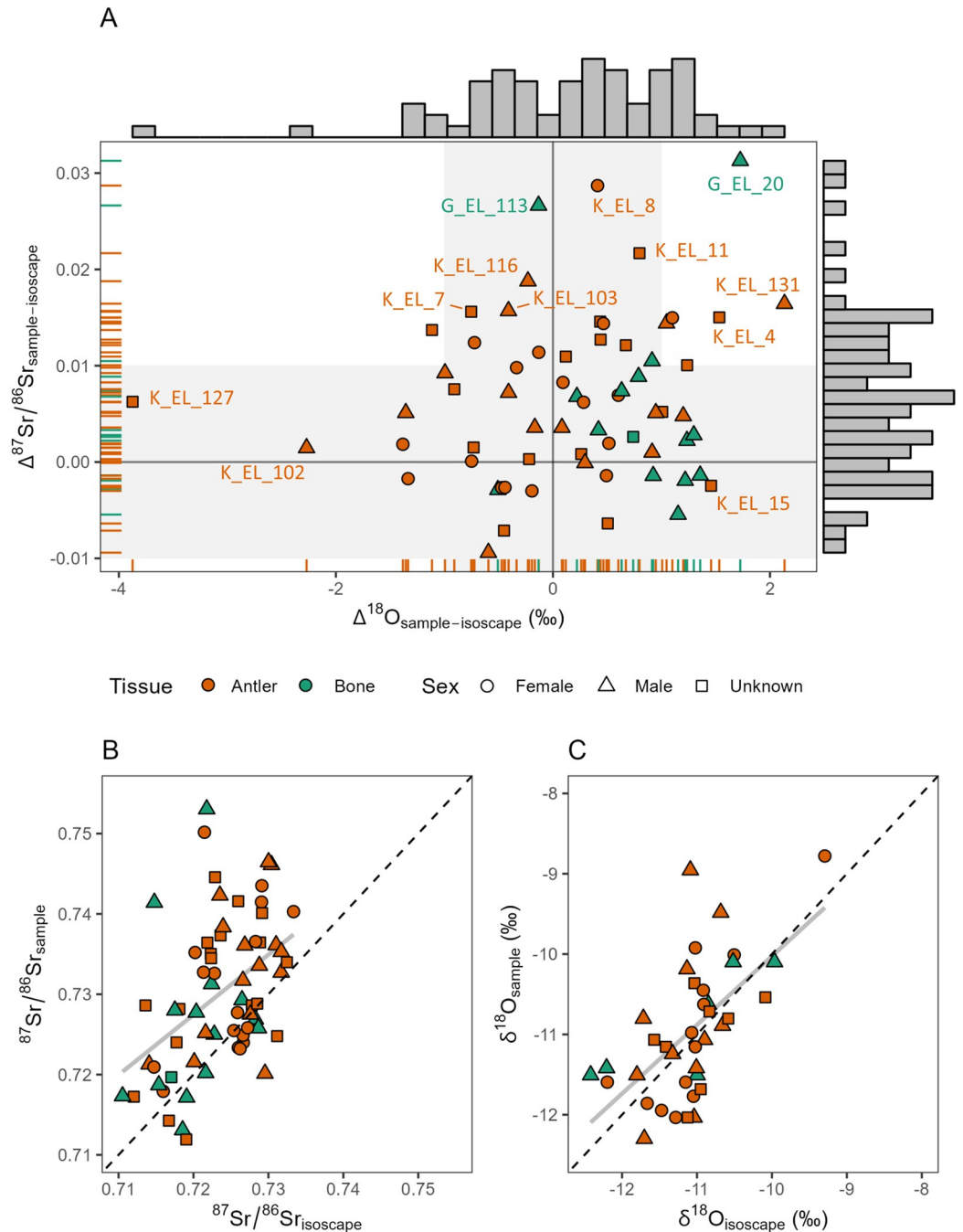
Fig 4. Data comparison between sample and isoscape. A) Bone (n = 50) symbols are orange; while antler (n = 15) symbols are green; males (n = 29) are triangles; females (n = 17) are circles; individuals with unknown sex (n = 19) are squares. One antler is reported as 'sex unknown' being labelled as 'hermaphrodite' in the museum ID card (see S1 Table). 1σ-outliers are labelled; gray bars on the sides are histograms of univariate sample distribution for $\Delta^{87}Sr/^{86}Sr_{sample-isoscape}$ and $\Delta^{18}O_{sample-isoscape}$; rug bars are also sample distributions but classified by sample type (bone and antler). Light grey areas are approximate median spatial uncertainties of the isoscapes ($\sim$0.01 for Sr and 1‰ for oxygen) depicted below and above $\Delta = 0$. B) The linear fit (1σ-outliers included) between the $^{87}Sr/^{86}Sr_{sample}$ and the $^{87}Sr/^{86}Sr_{isoscape}$ shows an R^2 of 0.20, $p < 0.01$; C) The linear fit (1σ-outliers included) between the $\delta^{18}O_{sample}$ (water) and the $\delta^{18}O_{isoscape}$ shows an R^2 of 0.30, $p < 0.01$.

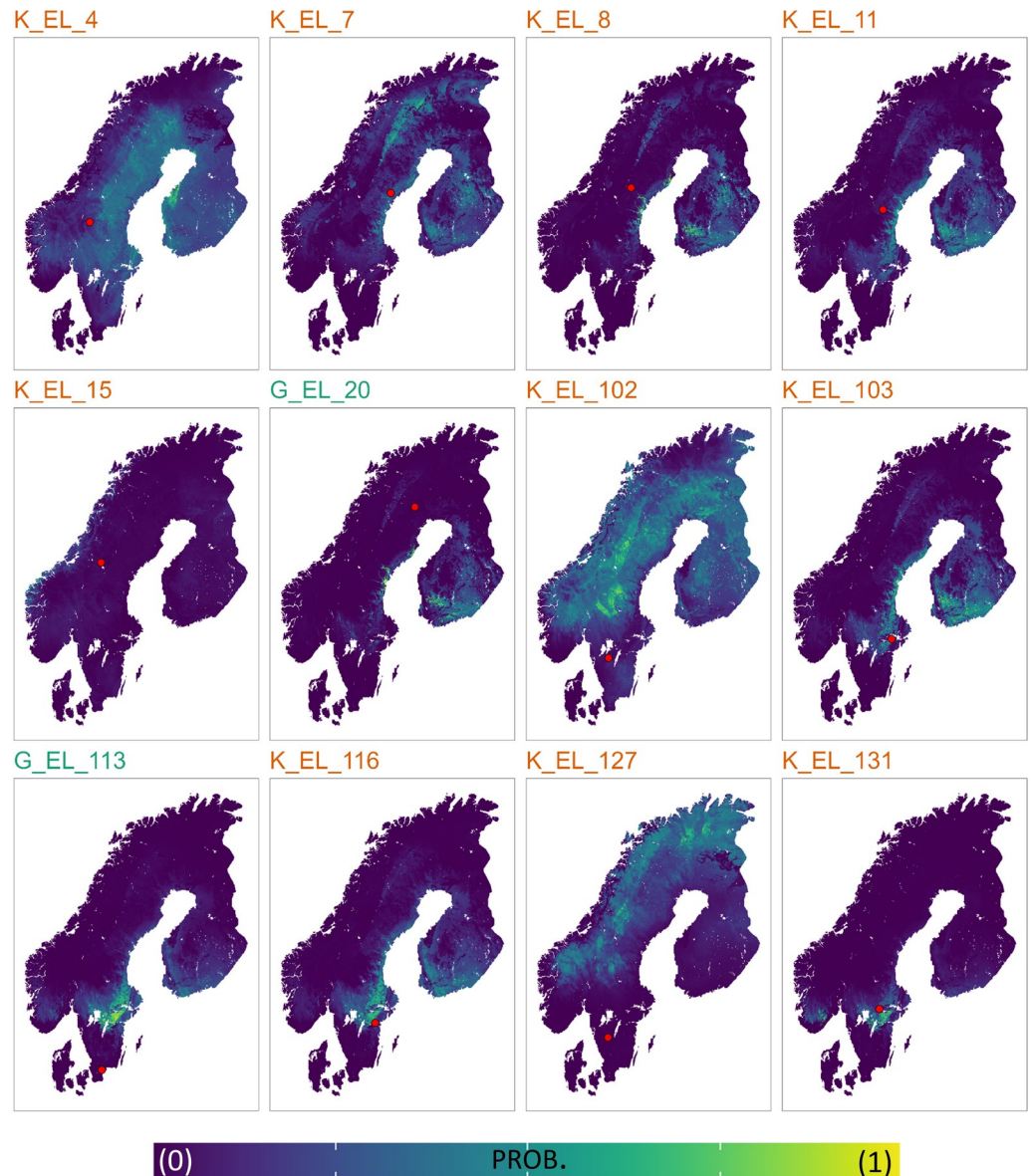https://doi.org/10.1371/journal.pone.0300867.g004

Fig 5. Moose provenance probabilities estimated through a Bayesian approach. Sr and O calibrated isoscapes were combined to predict the place of origin of the 1σ-outliers (see the Materials and Methods section). Red dots are the places of death of the individuals. Probability estimates are scaled between 0 (low probability, purple) and 1 (high probability, yellow). Sample's names are reported in green for antlers and orange for bones.

https://doi.org/10.1371/journal.pone.0300867.g005

of species are necessary to enable the conservation of biodiversity and ecosystems [8, 10]. Geochemistry is proving to be a key element in this regard, allowing to track animal movement across the territory. More and more isotopic landscapes have been built in recent years, both for archaeological and ecological applications [131, 145–149].

The newly built Sr isoscape of Scandinavia presented here fits in this research framework, with the goal of tracking moose movements across the landscape. The bedrock age has been shown to be key in controlling the bioavailable $^{87}Sr/^{86}Sr$ across Scandinavia. The most radiogenic Sr isotope compositions correspond to areas where Precambrian rocks, particularly those of the Svecofennian orogeny, outcrop that is in most of northern and central Sweden
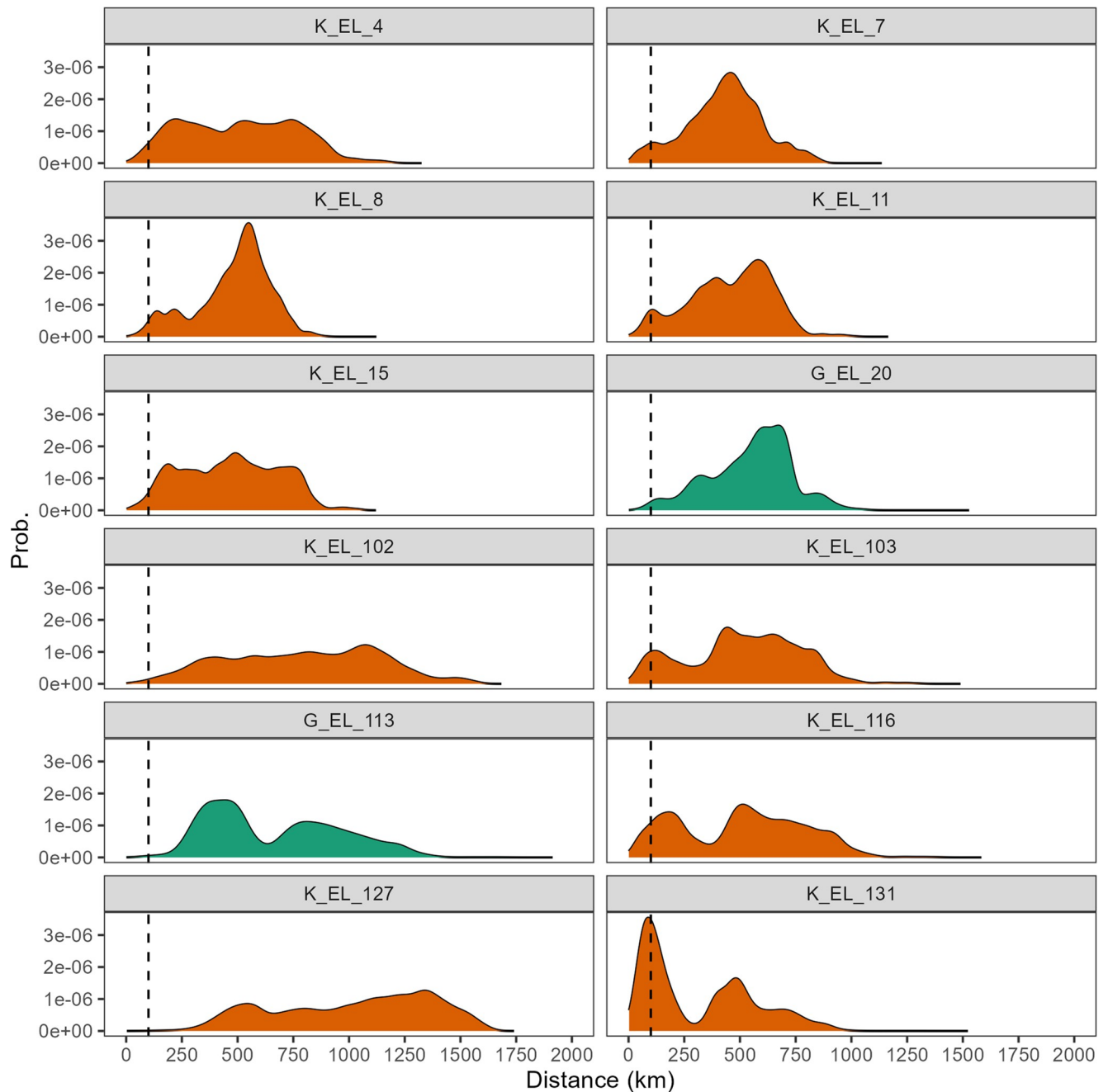
Fig 6. Probability distance of origin. Probability density plots representing the likely distance of movements determined for 1σ-outliers (see the Materials and Methods section) using *assignR* on the calibrated isoscapes. Bones are orange; antlers are green. Dashed line is an arbitrary cut-off value of 100 km (see Discussion).

and in southwestern Finland. The Sr isotope composition gradually becomes less radiogenic towards the west, across the Caledonides and down to the Norwegian coast line. The rocks of the Caledonides are clearly not only younger, but also contain ophiolitic sequences that generally have more depleted isotopic compositions. Along the coast of Norway, a key variable is the salt deposition through sea spray effects. Salts here are continuously replenished by oceanic waters. Interestingly, sea salt contribution is none in the Baltic Sea coastal regions most likely

due to the competing and major contribution of high Sr isotope signatures from the erosion of the outcropping Precambrian rocks.

It is well known that moose display a wide range of movements (migration, nomadism, dispersal, home range, sedentary) [47, 54, 150]. Variations in movements are visible at the population level (i.e., some individuals migrate while others do not), but also during the lifetime of a single individual (e.g., in relation to age). Many reasons were identified by scholars for moose movements in Scandinavia, including seasonality, forage availability and nutritional needs, climatic factors, snow depth and quality, sex differences (e.g., reproductive status, presence of calves), habitat deterioration, human presence in the landscape [46, 47, 56, 59, 60, 63, 65, 151]. So far, the usefulness of genetic analysis as an adjunct to ecological research has been highlighted [81, 82]. Geochemical analyses can add new and complementary information on moose mobility behaviour, both at a seasonal (antlers) and at annual level (bones).

We first note that the isotopic values of bones (mainly cranial bone) represent a mean of several years of life of the individual. On the other hand, the antlers provide an isotopic signal corresponding to their growing season (between spring and summer) [69, 152, 153]. In the present study, antlers were sampled close to the base, thus likely reflecting ~ 1 month of life in spring. Sr and O data of most of the moose samples (within 1σ-interval of $\Delta^{87}Sr/^{86}Sr_{sample\text{-}isoscape}$ and $\Delta^{18}O_{sample\text{-}isoscape}$) are likely compatible with the isotopic signature of the place of death, thus indicating a narrow home range. The 1σ-outliers whose provenance through the calibrated Sr-O isoscapes has been estimated include ten bones and two antlers (see Figs 5 and 6). Although in some cases the probability peaks begin to increase around 250 km away from the place of death and some samples display the highest peaks around 500 km distance, in the light of the ecological data on this animal (see below) it is reasonable to assume that the likely distance travelled is represented by the probability peaks between 0 and 100 km (see dashed line in Fig 6). However, it is possible that at least some individuals travelled longer distances (i.e., above 100 km; see Fig 6).

Available information on moose annual home range in Scandinavia shows that both migratory and nonmigratory individuals can travel mean maximum distances of approximately 5 to 28 km (diagonal of hypothetical square-shaped home ranges 12.6 and 410 km^2) [50, 58–61, 154, 155]. Similar values have also been documented in Canada and the United States, where the maximum distance travelled, obtained from annual home ranges of 20 to 300 km^2, spans from 6.3 to 24.4 km [156–161]. On the other hand, spring and summer home ranges of both migratory and nonmigratory moose in Scandinavia are reported to be from less than 1 to about 30 km^2, corresponding to a mean maximum distance travelled of 1.2 to 7.7 km [60, 61, 63, 162]. Higher distances have been reported for Canada and the United States. Here moose occupy seasonal ranges above 20 km^2 and up to 600 km^2, corresponding to maximum distances of 7 to 17.3 km [57, 156, 159].

During spring and fall migrations instead, moose in Sweden have been documented to travel a minimum of 4.4 up to 217 km [47, 163]. Migratory movements of 100 up to 500 km have been documented in Alaska, Siberia and Altai mountains [42, 164]. Long-distance dispersal of up to 1,500 km has been documented in the central United States [165]. Moose migrations over long distances have been confirmed by genetic analysis in both Scandinavia and continental Europe, showing a statistically significant gene flow at 300–400 km and 400–500 km, respectively [82]. In this sense, our most interesting samples are G_EL_113 (antler) and K_EL_127 (bone). Their probability distance of origin begins to increase from 250 km, reflecting larger-scale movements both seasonally (spring/summer) and annually. We emphasize here that G_EL_113 (non-local) provenance mainly relies on a remarkably high radiogenic Sr isotope value of the sample. As reported in the geostatistical framework section, the Sr Scandinavian isoscape shows the highest prediction uncertainties in high radiogenic areas and,

thus, we interpret the provenance of this sample with caution. Overall, more work is needed to accurately link the $^{87}Sr/^{86}Sr$ ratio of moose with Scandinavian bioavailable Sr baselines. This, in turn, indicates a need for more bioavailable Sr samples from radiogenic areas, as well as better statistical methods to estimate uncertainty in such highly variable regions.

Migratory patterns in moose can differ between male and female individuals. In our dataset, differences between the sexes are negligible. Although female moose are less represented, it is noteworthy that 6 out of 12 of the 1σ-outliers are males. The others are 1 female and 5 of unknown sex. This likely higher rate of movement of males than females agrees with the ecological data. Indeed, many scholars have found sexual differences in home range size and migration distance, both in relation to age and nutritional demand, with males travelling farther than females [47, 54, 60, 155].

Due to the remarkable implications of this approach for paleoecological and archaeological studies in Scandinavia, we tested our calibrated Sr isoscape on Swedish archaeological materials. We assessed the provenance of two moose samples from the Mesolithic Kanaljorden site in Motala previously published by Eriksson and colleagues [166]. These samples consist of a tooth pendant ($^{87}Sr/^{86}Sr$ = 0.72086) and an incisor ($^{87}Sr/^{86}Sr$ = 0.73489) defined as local and non-local to the site, respectively. The main issue with this assessment is that it was made using a local Sr baseline defined primarily by soil leachates. The leachable fraction of soils can be indeed less radiogenic (i.e., shifted to the local carbonate pool) than the local bioavailable $^{87}Sr/^{86}Sr$ [167]. For this reason, we propose that the $^{87}Sr/^{86}Sr$ local baseline assessed by Eriksson *et al.* [166] is possibly underestimated. Using our calibrated isoscape the provenance of the two moose samples changes. The more radiogenic incisor (Kanaljorden_2) appears to be local to the site, while the less radiogenic tooth pendant (Kanaljorden_1) is probably of non-local origin and compatible with an area about 100 km south of the site (Fig 7).

5.2 Carbon isotopes: Diet

Other key aspects of moose ecology, feeding habits and habitat selection, can be revealed by carbon stable isotopes [67, 69]. The mean $\delta^{13}C_{VPDB}$ values (corrected for the 'Suess effect') of the carbonate portion of bioapatite of our moose samples was -14.9‰ ($\pm$1.1‰) and -16.2‰ ($\pm$1.1‰) for antlers and bones, respectively. These values are typical of C_3 plants feeders, in agreement with the dominance of C_3 plants in the temperate and boreal environments of Europe [21, 100, 104, 141]. Since in these areas it is not possible to determine the type of plant consumed by herbivores (i.e., to discriminate between C_3 and C_4 plants with different photosynthetic pathways), the small differences in the $\delta^{13}C$ become crucial in identifying differences in C_3 plant-based diet due to climatic and environmental factors [68, 168], helping to obtain a more complete picture of moose ecology.

Interestingly, our antler samples display higher $\delta^{13}C$ values than bones. The first possible explanation for this difference can be related to seasonal variation in diet. Similar results were obtained by Kielland [67] for North American elk (*Alces alces gigas*) hooves, where winter values were ^{13}C-depleted compared to summer. Similarly, Walter and Leslie [169] found a relative increase of $\delta^{13}C$ values in the summer-portion of elk hooves (*Cervus elaphus*) from the Rocky Mountains and they interpreted this enrichment as a stronger reliance on C_4 grasses compared to winter. This, however, is unlikely for Sweden considering that the proportion of C_4 plants is close to 0% of the total plant species [141, 170, 171]. Moose are selective browsers feeding on a wide variety of plant species, with geographic and (intra)seasonal differences [41, 158, 172]. The foraging behaviour has been shown to depend both on food availability (which influences selectivity) and nutritional requirements, two aspects also influencing spring and fall migrations [48, 173–177]. In spring and summer, during the growing season of both plants and antlers, moose
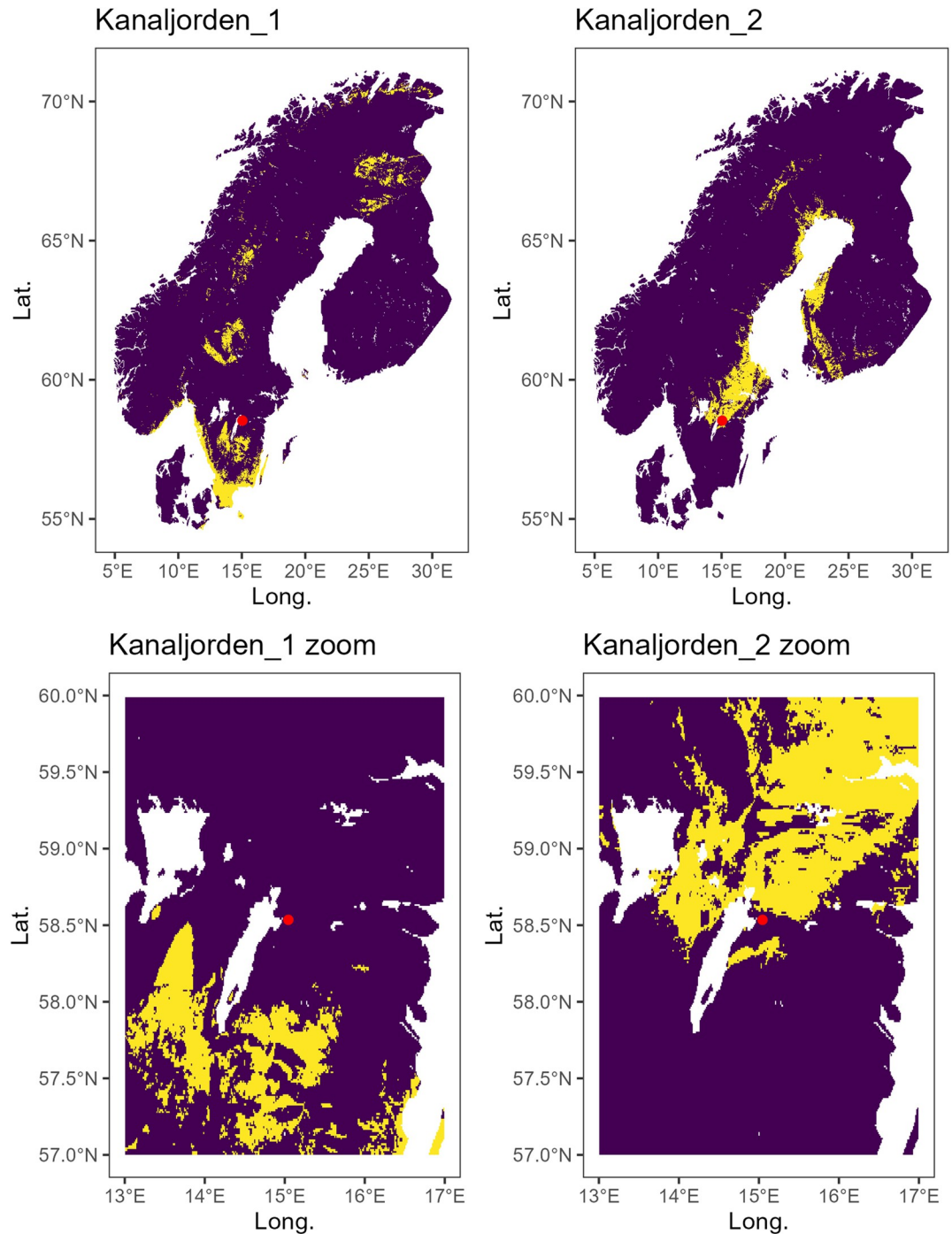
Fig 7. Top 5% probability of origin of two archaeological moose samples based on their Sr isotope ratio. Sample Kanaljorden_1 is a tooth pendant (enamel $^{87}Sr/^{86}Sr$ = 0.72086) while Kanaljorden_2 is an incisor (enamel $^{87}Sr/^{86}Sr$ = 0.73489). Data are from Eriksson *et al.* [166]. The red dot is the site of Kanaljorden. Yellow represents highly probable areas of origin (top 5%, see [138]), while purple represents low probable areas of origin.

https://doi.org/10.1371/journal.pone.0300867.g007

can rely on more high-quality food than in winter. The main diet components are shoots and leaves of young trees and shrubs, but also herbs, grasses and aquatic plants when available [158, 172, 178]. Preferred species are deciduous trees such as willow (*Salix* spp.), birches (*Betula*

spp.), aspen (*Populus tremula*) and rowan (*Sorbus aucuparia*), but also ground vegetation released from snow such as blueberry (*Vaccinum myrtillus*) [163, 175, 176, 179]. During winter (the dormant period) moose preferentially feed on twigs and bark of the same deciduous browse species (lignin is $\sim 3‰$ ^{13}C-depleted compared to leaves, [180]), but also rely on conifers, especially the widely distributed Scots pine (*Pinus sylvestris*) [42, 50, 61, 63, 173, 177, 179, 181].

The "Canopy effect" [102, 103] could also have contributed to $\delta^{13}C$ values in our samples, which is known to be detectable in the $\delta^{13}C$ values of large herbivores dwelling in forested environments of boreal and temperate ecosystems [182]. Forest cover has been found to be the main factor influencing the wide variability of $\delta^{13}C$ in modern moose samples from Europe [68]. Our data do not support the canopy effect as the main driving factor for differences in $\delta^{13}C$ values between bones and antlers, and in general to the observed $\delta^{13}C$ variability; yet, we need to stress that the moose samples analysed in this study date between the 1800 and 1994, so changes in forest cover through time might have biased our estimations. Moreover, an increased forest cover during warm seasons would have shown an inverse pattern in $\delta^{13}C$ values, i.e., antlers depleted compared to bones. In terms of moose ethology, seeking forest cover is documented throughout the year to find shelter from both predators (including humans) and environmental conditions. During winter moose seek forest cover to find shelter from wind and snow (which in open environments limits access to forage). During summer they tend to avoid open habitats and use areas with dense canopies to cope with high temperatures, especially when above 20˚C [158, 183, 184].

Overall, the differences in $\delta^{13}C$ between moose bones and antlers likely result from a combination of factors. Moose display a complex foraging behaviour that changes seasonally according to mobility, nutritional requirements, food availability and environmental factors [61, 63, 150, 158, 173, 175]. Besides, we cannot exclude eventual sub-annual fluctuations in atmospheric CO_2 isotope composition as a possible driving factor for $\delta^{13}C$ in moose tissues [185]. In addition, the consumption of lipids may shift the $\delta^{13}C$ values of tissues toward more negative values, e.g., during periods of metabolic stress. Assuming possible winter stress of moose due to limited food resources, lower $\delta^{13}C$ values in year-round remodelling bones compared to spring-summer growing antlers and can be partially explained by an increased catabolism of endogenous fat reserves during the winter season (see e.g., [186]).

6. Conclusion and future perspectives

We report here a dataset of strontium ($^{87}Sr/^{86}Sr$), oxygen ($\delta^{18}O$) and carbon ($\delta^{13}C$) isotope values of modern moose bones and antlers from Sweden. This is the largest database of moose isotope values presented so far for the area and can be used for future research in *Alces* sp. (palaeo)ecology and in general as a modern reference dataset for mammal isotope compositions of Scandinavia. However, our samples and their metadata come from individuals collected during the 19th century and, as such, we cannot be fully confident in their geographic assignment and dating. This is a common problem when dealing with samples from historic collections (see e.g. [187]). Nevertheless, most of the moose samples here considered are compatible with the local predicted isotope baseline, reinforcing the hypothesis of a correct geographic assignment.

We compiled bioavailable Sr isotope data from literature and used them to build the first Sr isoscape of whole Scandinavia using a machine learning approach. Even if additional bioavailable Sr isotope samples will further improve its predictive power, the Sr isoscape presented herein can be a useful tool for provenance studies in the area (both for modern and archaeological faunal or human samples, but also for foods, artefacts and plant materials).

After comparison with the constructed isoscapes, the seasonal (antler) and multi-annual (bone) mobility assessed through the workflow presented in this paper agrees well with ecological data on moose movement behaviour (i.e., home-range, migration). Even if there are some limiting factors to our interpretation (i.e., errors associated with the isoscape in S6 Fig and a likely biased representation of moose diet in the isoscape, see Results), the Bayesian workflow presented here will provide a better understanding of how moose move across the Scandinavian landscape, and become a useful mean to support traditional mobility tracking methods (e.g., radio-, satellite- and GPS-tracking) and genetic analyses. Future work combining animal tracking with isotope analysis will advance our understanding of the relationship between isotope values and animal behaviour.

The $\delta^{13}C$ values are typical of C_3 plant feeders, and the differences detected between antlers (^{13}C-enriched) and bones (^{13}C-depleted) are likely due to seasonal differences in dietary habits and/or physiological stress during winter. Sub-annual fluctuations of atmospheric CO_2 levels may also have affected the $\delta^{13}C$ values of moose. However, further work is needed (i.e., high-resolution sampling/analyses) to precisely understand winter-summer isotopic differences in moose hard tissues to interpret their diet and physiology in a comprehensive way.

In our view, especially in light of the growing concern about the effects of climate change on animal migration and biodiversity conservation, geochemical analyses should become an integral part of multidisciplinary studies aimed at reconstructing wildlife mobility.

Supporting information

S1 Fig. (A) Calculated intra-site (i.e. same coordinates' samples) standard deviations for literature values used in building the isoscape vs. their mean isotope values. (B) Extrapolated RF error (from the error map) at the same sites vs. the mean isotope values as in A. (C) Calculated intra-site standard deviations for literature values vs. extrapolated RF error. See Materials and Methods for discussion.
(DOCX)

S2 Fig. Random forest model performances. (A) Modelled Sr isotope ratios vs observed Sr isotope ratios of isoscape samples; the 10-fold cross-validation resulted in an RMSE = 0.0055 and an R^2 = 0.65. (B) Variable importance of the seven external predictors (r.srsrq3, r.fert, r.elevation, r.ssa, r.cec, r.ssaw and r.mat) selected by using the VSURF algorithm. See Bataille et al. (2020) for details. (C) Partial dependence plot for the VSURF-selected variables.
(DOCX)

S3 Fig. $\Delta^{87}Sr/^{86}Sr_{sample-isoscape}$ and $\Delta^{18}O_{sample-isoscape}$ plotted over the Scandinavia map.
(DOCX)

S4 Fig. $\Delta^{87}Sr/^{86}Sr_{sample-isoscape}$ and $\Delta^{18}O_{sample-isoscape}$ plotted vs individual sex. Only samples of known sex were considered.
(DOCX)

S5 Fig. Difference between calibrated-uncalibrated Sr (A) and O (B) isoscapes. Calibrated isoscapes were obtained by using Δs of moose samples within 1σ (see the main text for details).
(DOCX)

S6 Fig. Sr isoscape (RF model) error map. The calculation was carried out as reported in the Materials and Methods section of the main text.
(DOCX)

S1 Table. Moose samples' data.
(XLSX)

S2 Table. Literature values used to build the Scandinavia isoscape.
(XLSX)

S3 Table. Coefficients of determination of sample vs isoscape isotope ratio regression. P values are always $\ll 0.01$.
(XLSX)

S1 File. Sr isoscape of Scandinavia as GeoTIFF.
(TIF)

S2 File. Sr uncertainty map of Scandinavia as GeoTIFF.
(TIF)

Acknowledgments

Author Contributions

Conceptualization: Elena Armaroli, Federico Lugli, Anna Cipriani, Thomas Tütken.

Data curation: Elena Armaroli, Federico Lugli.

Formal analysis: Elena Armaroli, Federico Lugli, Anna Cipriani, Thomas Tütken.

Funding acquisition: Anna Cipriani, Thomas Tütken.

Investigation: Elena Armaroli, Federico Lugli, Anna Cipriani, Thomas Tütken.

Methodology: Elena Armaroli, Federico Lugli, Anna Cipriani, Thomas Tütken.

Project administration: Anna Cipriani, Thomas Tütken.

Resources: Anna Cipriani, Thomas Tütken.

Software: Federico Lugli.

Supervision: Federico Lugli, Anna Cipriani, Thomas Tütken.

Validation: Elena Armaroli, Federico Lugli.

Visualization: Elena Armaroli, Federico Lugli.

Writing – original draft: Elena Armaroli, Federico Lugli.

Writing – review & editing: Elena Armaroli, Federico Lugli, Anna Cipriani, Thomas Tütken.

References

1. Massol F, Gravel D, Mouquet N, Cadotte MW, Fukami T, Leibold MA. Linking community and ecosystem dynamics through spatial ecology: An integrative approach to spatial food webs. Ecol Lett. 2011; 14: 313–323. https://doi.org/10.1111/j.1461-0248.2011.01588.x PMID: 21272182

2. Fletcher R, Fortin M-J. Introduction to spatial ecology and its relevance for conservation. Spatial Ecology and Conservation Modeling: Applications with R. Cham: Springer International Publishing; 2018. pp. 1–13. https://doi.org/10.1007/978-3-030-01989-1_1

3. Pressey RL, Cabeza M, Watts ME, Cowling RM, Wilson KA. Conservation planning in a changing world. Trends Ecol Evol. 2007; 22: 583–592. https://doi.org/10.1016/j.tree.2007.10.001 PMID: 17981360

4. Mawdsley JR, O'Malley R, Ojima DS. A review of climate-change adaptation strategies for wildlife management and biodiversity conservation. Conserv Biol. 2009; 23: 1080–1089. https://doi.org/10.1111/j.1523-1739.2009.01264.x PMID: 19549219

5. Schmitz OJ, Lawler JJ, Beier P, Groves C, Knight G, Boyce DA, et al. Conserving biodiversity: Practical guidance about climate change adaptation approaches in support of land-use planning. Nat Areas J. 2015; 35: 190–203. https://doi.org/10.3375/043.035.0120

6. Carroll C, Roberts DR, Michalak JL, Lawler JJ, Nielsen SE, Stralberg D, et al. Scale-dependent complementarity of climatic velocity and environmental diversity for identifying priority areas for conservation under climate change. Glob Change Biol. 2017; 23: 4508–4520. https://doi.org/10.1111/gcb.13679 PMID: 28267245

7. Parmesan CPR. Ecological and evolutionary responses to recent climate change. Annu Rev Ecol Evol Syst. 2006; 37: 637–669. https://doi.org/10.1146/annurev.ecolsys.37.091305.110100

8. Sergio F, Blas J, Hiraldo F. Animal responses to natural disturbance and climate extremes: A review. Glob Planet Change. 2018; 161: 28–40. https://doi.org/10.1016/j.gloplacha.2017.10.009

9. Harris G, Thirgood S, Hopcraft J, Cromsight J, Berger J. Global decline in aggregated migrations of large terrestrial mammals. Endanger Species Res. 2009; 7: 55–76. https://doi.org/10.3354/esr00173

10. Allen AM, Singh NJ. Linking movement ecology with wildlife management and conservation. Front Ecol Evol. 2016; 3: 155. https://doi.org/10.3389/fevo.2015.00155

11. Araujo MB, Pearson RG, Thuiller W, Erhard M. Validation of species-climate impact models under climate change. Glob Change Biol. 2005; 11: 1504–1513. https://doi.org/10.1111/j.1365-2486.2005.01000.x

12. Harrison PA, Berry PM, Butt N, New M. Modelling climate change impacts on species' distributions at the European scale: implications for conservation policy. Environ Sci Policy. 2006; 9: 116–128. https://doi.org/10.1016/j.envsci.2005.11.003

13. Austin M. Species distribution models and ecological theory: A critical assessment and some possible new approaches. Ecol Model. 2007; 200: 1–19. https://doi.org/10.1016/j.ecolmodel.2006.07.005

14. Talluto MV, Boulangeat I, Ameztegui A, Aubin I, Berteaux D, Butler A, et al. Cross-scale integration of knowledge for predicting species ranges: A metamodelling framework. Glob Ecol Biogeogr. 2016; 25: 238–249. https://doi.org/10.1111/geb.12395 PMID: 27499698

15. Bolger DT, Newmark WD, Morrison TA, Doak DF. The need for integrative approaches to understand and conserve migratory ungulates. Ecol Lett. 2008; 11: 63–77. https://doi.org/10.1111/j.1461-0248.2007.01109.x PMID: 17897327

16. Shuman B. Patterns, processes, and impacts of abrupt climate change in a warm world: the past 11,700 years. Wiley Interdiscip Rev Clim Change. 2012; 3: 19–43. https://doi.org/10.1002/wcc.152

17. Izdebski A, Holmgren K, Weiberg E, Stocker SR, Büntgen U, Florenzano A, et al. Realising consilience: How better communication between archaeologists, historians and natural scientists can transform the study of past climate change in the Mediterranean. Quat Sci Rev. 2016; 136: 5–22. https://doi.org/10.1016/j.quascirev.2015.10.038

18. Mandel JT, Bohrer G, Winkler DW, Barber DR, Houston CS, Bildstein KL. Migration path annotation: Cross-continental study of migration-flight response to environmental conditions. Ecol Appl. 2011; 21: 2258–2268. https://doi.org/10.1890/10-1651.1 PMID: 21939059

19. Ericson JE. Strontium isotope characterization in the study of prehistoric human ecology. J Hum Evol. 1985; 14: 503–514. https://doi.org/10.1016/S0047-2484(85)80029-4

20. Bowen GJ, Wassenaar LI, Hobson KA. Global application of stable hydrogen and oxygen isotopes to wildlife forensics. Oecologia. 2005; 143: 337–348. https://doi.org/10.1007/s00442-004-1813-y PMID: 15726429

21. Kohn MJ. Carbon isotope compositions of terrestrial C_3 plants as indicators of (paleo)ecology and (paleo)climate. Proc Natl Acad Sci. 2010; 107: 19691–19695. https://doi.org/10.1073/pnas.1004933107 PMID: 21041671

22. Voerkelius S, Lorenz GD, Rummel S, Quétel CR, Heiss G, Baxter M, et al. Strontium isotopic signatures of natural mineral waters, the reference to a simple geological map and its potential for authentication of food. Food Chem. 2010; 118: 933–940. https://doi.org/10.1016/j.foodchem.2009.04.125

23. Brombin V, Natali C, Frijia G, Schmitt K, Casalini M, Bianchini G. Isotope geochemistry for seafood traceability and authentication: The northern Adriatic manila clams case study. Foods. 2022; 11: 3054. https://doi.org/10.3390/foods11193054 PMID: 36230130

24. Montgomery J. Passports from the past: Investigating human dispersals using strontium isotope analysis of tooth enamel. Ann Hum Biol. 2010; 37: 325–346. https://doi.org/10.3109/03014461003649297 PMID: 20367186

25. Sehrawat JS, Kaur J. Role of stable isotope analyses in reconstructing past life-histories and the provenancing human skeletal remains: A review. Anthropol Rev. 2017; 80: 243–258. https://doi.org/10.1515/anre-2017-0017

26. Pederzani S, Britton K. Oxygen isotopes in bioarchaeology: Principles and applications, challenges and opportunities. Earth-Sci Rev. 2019; 188: 77–107. https://doi.org/10.1016/j.earscirev.2018.11.005

27. Price TD, Bentley RA, Lüning J, Gronenborn D, Wahl J. Prehistoric human migration in the *Linearbandkeramik* of Central Europe. Antiquity. 2001; 75: 593–603. https://doi.org/10.1017/S0003598X00088827

28. Thornton EK. Reconstructing ancient Maya animal trade through strontium isotope ($^{87}Sr/^{86}Sr$) analysis. J Archaeol Sci. 2011; 38: 3254–3263. https://doi.org/10.1016/j.jas.2011.06.035

29. Makarewicz CA, Arbuckle BS, Öztan A. Vertical transhumance of sheep and goats identified by intra-tooth sequential carbon ($\delta^{13}C$) and oxygen ($\delta^{18}O$) isotopic analyses: Evidence from Chalcolithic Köşk Höyük, central Turkey. J Archaeol Sci. 2017; 86: 68–80. https://doi.org/10.1016/j.jas.2017.01.003

30. Kowalik N, Anczkiewicz R, Wilczyński J, Wojtal P, Müller W, Bondioli L, et al. Tracing human mobility in central Europe during the Upper Paleolithic using sub-seasonally resolved Sr isotope records in ornaments. Sci Rep. 2020; 10: 10386. https://doi.org/10.1038/s41598-020-67017-2 PMID: 32587350

31. Britton K, Grimes V, Dau J, Richards MP. Reconstructing faunal migrations using intra-tooth sampling and strontium and oxygen isotope analyses: A case study of modern caribou *(Rangifer tarandus granti)*. J Archaeol Sci. 2009; 36: 1163–1172. https://doi.org/10.1016/j.jas.2009.01.003

32. Kohn MJ, Schoeninger MJ, Barker WW. Altered states: Effects of diagenesis on fossil tooth chemistry. Geochim Cosmochim Acta. 1999; 63: 2737–2747. https://doi.org/10.1016/S0016-7037(99)00208-2

33. Hoppe KA, Koch PL, Furutani TT. Assessing the preservation of biogenic strontium in fossil bones and tooth enamel. Int J Osteoarchaeol. 2003; 13: 20–28. https://doi.org/10.1002/oa.663

34. Lewis J, Pike AWG, Coath CD, Evershed RP. Strontium concentration, radiogenic ($^{87}Sr/^{86}Sr$) and stable ($\delta^{88}Sr$) strontium isotope systematics in a controlled feeding study. STAR Sci Technol Archaeol Res. 2017; 3: 45–57. https://doi.org/10.1080/20548923.2017.1303124

35. Lüdecke T, Leichliter JN, Aldeias V, Bamford MK, Biro D, Braun DR, et al. Carbon, nitrogen, and oxygen stable isotopes in modern tooth enamel: A case study from Gorongosa National Park, central Mozambique. Front Ecol Evol. 2022; 10: 958032. https://doi.org/10.3389/fevo.2022.958032

36. Price TD, Burton JH, Bentley RA. The characterization of biologically available strontium isotope ratios for the study of prehistoric migration. Archaeometry. 2002; 44: 117–135. https://doi.org/10.1111/1475-4754.00047

37. Maurer A-F, Galer SJG, Knipper C, Beierlein L, Nunn EV, Peters D, et al. Bioavailable $^{87}Sr/^{86}Sr$ in different environmental samples—Effects of anthropogenic contamination and implications for isoscapes in past migration studies. Sci Total Environ. 2012; 433: 216–229. https://doi.org/10.1016/j.scitotenv.2012.06.046 PMID: 22796412

38. Bowen GJ. Isoscapes: Spatial pattern in isotopic biogeochemistry. Annu Rev Earth Planet Sci. 2010; 38: 161–187. https://doi.org/10.1146/annurev-earth-040809-152429

39. Bataille CP, von Holstein ICC, Laffoon JE, Willmes M, Liu X-M, Davies GR. A bioavailable strontium isoscape for Western Europe: A machine learning approach. PLOS ONE. 2018; 13: e0197386. https://doi.org/10.1371/journal.pone.0197386 PMID: 29847595

40. Bataille CP, Crowley BE, Wooller MJ, Bowen GJ. Advances in global bioavailable strontium isoscapes. Palaeogeogr Palaeoclimatol Palaeoecol. 2020; 555: 109849. https://doi.org/10.1016/j.palaeo.2020.109849

41. Franzmann AW. Alces alces. Mamm Species. 1981; 154: 1–7. https://doi.org/10.2307/3503876

42. Baskin L, Danell K. Moose—*Alces alces*: *Alces alces* Linnaeus, 1758. Artiodactyla, Cervidae, Odocoileinae. Ecology of Ungulates: A Handbook of Species in Eastern Europe and Northern and Central Asia. Berlin, Heidelberg: Springer Berlin Heidelberg; 2003. pp. 91–108. https://doi.org/10.1007/978-3-662-06820-5

43. Schmölcke U, Zachos FE. Holocene distribution and extinction of the moose (*Alces alces*, Cervidae) in Central Europe. Mamm Biol. 2005; 70: 329–344. https://doi.org/10.1016/j.mambio.2005.08.001

44. Niedziałkowska M, Hundertmark KJ, Jędrzejewska B, Niedziałkowski K, Sidorovich VE, Gòrny M, et al. Spatial structure in European moose (Alces alces): Genetic data reveal a complex population history. J Biogeogr. 2014; 41: 2173–2184. https://doi.org/10.1111/jbi.12362

45. Niedziałkowska M. Phylogeography of European moose (*Alces alces*) based on contemporary mtDNA data and archaeological records. Mamm Biol. 2017; 84: 35–43. https://doi.org/10.1016/j.mambio.2017.01.004

46. van Beest FM, Rivrud IM, Loe LE, Milner JM, Mysterud A. What determines variation in home range size across spatiotemporal scales in a large browsing herbivore? J Anim Ecol. 2011; 80: 771–785. https://doi.org/10.1111/j.1365-2656.2011.01829.x PMID: 21388373

47. Singh NJ, Börger L, Dettki H, Bunnefeld N, Ericsson G. From migration to nomadism: Movement variability in a northern ungulate across its latitudinal range. Ecol Appl. 2012; 22: 2007–2020. https://doi.org/10.1890/12-0245.1 PMID: 23210316

48. Hörnberg S. Changes in population density of moose (*Alces alces*) and damage to forests in Sweden. For Ecol Manag. 2001; 149: 141–151. https://doi.org/10.1016/S0378-1127(00)00551-X

49. Sylvén S. Management and regulated harvest of moose (*Alces alces*) in Sweden. Uppsala: Swedish Univ. of Agricultural Sciences; 2003.

50. Cassing G, Greenberg LA, Mikusiñski G. Moose (*Alces alces*) browsing in young forest stands in central Sweden: A multiscale perspective. Scand J For Res. 2006; 21: 221–230. https://doi.org/10.1080/02827580600673535

51. Månsson J, Hauser CE, Andrén H, Possingham HP. Survey method choice for wildlife management: The case of moose *Alces alces* in Sweden. Wildl Biol. 2011; 17: 176–190. https://doi.org/10.2981/10-052

52. Salisbury J, Hu X, Speed JDM, Iordan CM, Austrheim G, Cherubini F. Net climate effects of moose browsing in early successional boreal forests by integrating carbon and albedo dynamics. J Geophys Res Biogeosciences. 2023; 128: e2022JG007279. https://doi.org/10.1029/2022JG007279

53. Lavsund S, Nygrén T, Solberg EJ. Status of moose populations and challenges to moose management in Fennoscandia. Alces J Devoted Biol Manag Moose. 2003; 39: 109–130.

54. Bunnefeld N, Börger L, van Moorter B, Rolandsen CM, Dettki H, Solberg EJ, et al. A model-driven approach to quantify migration patterns: individual, regional and yearly differences: Quantifying migration patterns. J Anim Ecol. 2011; 80: 466–476. https://doi.org/10.1111/j.1365-2656.2010.01776.x PMID: 21105872

55. Singh NJ, Milner-Gulland EJ. Conserving a moving target: Planning protection for a migratory species as its distribution changes: Landscape-scale planning for a migratory species. J Appl Ecol. 2011; 48: 35–46. https://doi.org/10.1111/j.1365-2664.2010.01905.x

56. Ball JP, Nordengren C, Wallin K. Partial migration by large ungulates: Characteristics of seasonal moose *Alces alces* ranges in northern Sweden. Wildl Biol. 2001; 7: 39–47. https://doi.org/10.2981/wlb.2001.007

57. White KS, Barten NL, Crouse S, Crouse J. Benefits of migration in relation to nutritional condition and predation risk in a partially migratory moose population. Ecology. 2014; 95: 225–237. https://doi.org/10.1890/13-0054.1 PMID: 24649661

58. Eriksen A, Wabakken P, Zimmermann B, Andreassen HP, Arnemo JM, Gundersen H, et al. Activity patterns of predator and prey: A simultaneous study of GPS-collared wolves and moose. Anim Behav. 2011; 81: 423–431. https://doi.org/10.1016/j.anbehav.2010.11.011

59. Wikenros C, Balogh G, Sand H, Nicholson KL, Månsson J. Mobility of moose-comparing the effects of wolf predation risk, reproductive status, and seasonality. Ecol Evol. 2016; 6: 8870–8880. https://doi.org/10.1002/ece3.2598 PMID: 28035275

60. Cederlund G, Sand H. Home-range size in relation to age and sex in moose. J Mammal. 1994; 75: 1005–1012. https://doi.org/10.2307/1382483

61. Cederlund GN, Okarma H. Home range and habitat use of adult female moose. J Wildl Manag. 1988; 52: 336–343. https://doi.org/10.2307/3801246

62. Lundmark C, Ball JP. Living in snowy environments: Quantifying the influence of snow on moose behavior. Arct Antarct Alp Res. 2008; 40: 111–118. https://doi.org/10.1657/1523-0430(06–103)[LUNDMARK]2.0.CO;2

63. Cederlund G, Bergström R, Sandegren F. Winter activity patterns of females in two moose populations. Can J Zool. 1989; 67: 1516–1522. https://doi.org/10.1139/z89-216

64. Andersen R. Habitat deterioration and the migratory behaviour of moose (*Alces alces* L.) in Norway. J Appl Ecol. 1991; 28: 102–108. https://doi.org/10.2307/2404117

65. Andersen R. Habitat changes in moose ranges: Effects on migratory behavior, site fidelity and size of summer home-range. Alces J Devoted Biol Manag Moose. 1991; 27: 85–92.

66. Ben-David M, Shochat E, Adams LG. Utility of stable isotope analysis in studying foraging ecology of herbivores: Examples from moose and caribou. Alces J Devoted Biol Manag Moose. 2001; 37: 421–434.

67. Kielland K. Stable isotope signatures of moose in relation to seasonal forage composition: A hypothesis. Alces J Devoted Biol Manag Moose. 2001; 37: 329–337.

68. Hofman-Kamińska E, Bocherens H, Borowik T, Drucker DGG, Kowalczyk R. Stable isotope signatures of large herbivore foraging habitats across Europe. PLoS ONE. 2018; 13: e0190723. https://doi.org/10.1371/journal.pone.0190723 PMID: 29293647

69. Schwartz-Narbonne R, Plint T, Hall E, Zazula G, Longstaffe FJ. Seasonal paleoecological records from antler collagen δ^{13}C and δ^{15}N. Paleobiology. 2021; 47: 533–549. https://doi.org/10.1017/pab.2021.1

70. Groves P, Mann DH, Kunz ML. Prehistoric perspectives can help interpret the present: 14 000 years of moose (*Alces alces*) in the Western Arctic. Can J Zool. 2022; 100: 732–746. https://doi.org/10.1139/cjz-2022-0079

71. Sjögren K-G, Price TD, Ahlström T. Megaliths and mobility in south-western Sweden. Investigating relationships between a local society and its neighbours using strontium isotopes. J Anthropol Archaeol. 2009; 28: 85–101. https://doi.org/10.1016/j.jaa.2008.10.001

72. Frei KM, Price TD. Strontium isotopes and human mobility in prehistoric Denmark. Archaeol Anthropol Sci. 2012; 4: 103–114. https://doi.org/10.1007/s12520-011-0087-7

73. Bläuer A, Korkeakoski-Väisänen K, Arppe L, Kantanen J. Bronze age cattle teeth and cremations from a monumental burial cairn in Selkäkangas, Finland: New radiocarbon dates and isotopic analysis. Est J Archaeol. 2013; 17: 3–23. https://doi.org/10.3176/arch.2013.1.01

74. Price TD, Naumann E. The peopling of the North Atlantic: Isotopic results from Norway. J N Atl. 2014; 7: 88–102. https://doi.org/10.3721/037.002.sp706

75. Kjällquist M, Price TD. Mesolithic mobility and social contact networks in south Scandinavia around 7000 BCE: Lithic raw materials and isotopic proveniencing of human remains from Norje Sunnansund, Sweden. J Anthropol Archaeol. 2019; 53: 186–201. https://doi.org/10.1016/j.jaa.2018.12.007

76. Blank M, Sjögren K-G, Knipper C, Frei KM, Malmström H, Fraser M, et al. Mobility patterns in inland southwestern Sweden during the Neolithic and Early Bronze Age. Archaeol Anthropol Sci. 2021; 13: 1–32. https://doi.org/10.1007/s12520-021-01294-4

77. Price TD, Klassen L, Sjögren K-G. Pitted ware culture: Isotopic evidence for contact between Sweden and Denmark across the Kattegat in the Middle Neolithic, ca. 3000 BC. J Anthropol Archaeol. 2021; 61: 101254. https://doi.org/10.1016/j.jaa.2020.101254

78. Price TD, Frei KM, Naumann E. Isotopic baselines in the North Atlantic region. J N Atl. 2014; 7: 103–136. https://doi.org/10.3721/037.002.sp707

79. Blank M, Sjögren K-G, Knipper C, Frei KM, Storå J. Isotope values of the bioavailable strontium in inland southwestern Sweden—A baseline for mobility studies. PLOS ONE. 2018; 13: e0204649. https://doi.org/10.1371/journal.pone.0204649 PMID: 30286158

80. Ladegaard-Pedersen P, Sabatini S, Frei R, Kristiansen K, Frei KM. Testing Late Bronze Age mobility in southern Sweden in the light of a new multi-proxy strontium isotope baseline of Scania. PLOS ONE. 2021; 16: e0250279. https://doi.org/10.1371/journal.pone.0250279 PMID: 33882110

81. Finnegan LA, Wilson PJ, Price GN, Lowe SJ, Patterson BR, Fortin M-J, et al. The complimentary role of genetic and ecological data in understanding population structure: A case study using moose (*Alces alces*). Eur J Wildl Res. 2012; 58: 415–423. https://doi.org/10.1007/s10344-011-0590-2

82. Niedziałkowska M, Jędrzejewska B, Danyłow J, Niedziałkowski K. Diverse rates of gene flow and long-distance migration in two moose *Alces alces* subpopulations in Europe. Mammal Res. 2016; 61: 171–178. https://doi.org/10.1007/s13364-016-0274-0

83. Crowley BE, Bataille CP, Haak BA, Sommer KM. Identifying nesting grounds for juvenile migratory birds with dual isotope: An initial test using North American raptors. Ecosphere. 2021; 12: e03765. https://doi.org/10.1002/ecs2.3765

84. Bentley RA. Strontium isotopes from the Earth to the archaeological skeleton: A review. J Archaeol Method Theory. 2006; 13: 135–187. https://doi.org/10.1007/s10816-006-9009-x

85. Capo RC, Stewart BW, Chadwick OA. Strontium isotopes as tracers of ecosystem processes: Theory and methods. Geoderma. 1998; 82: 197–225. https://doi.org/10.1016/S0016-7061(97)00102-X

86. Graustein WC. ^{87}Sr/^{86}Sr ratios measure the sources and flow of strontium in terrestrial ecosystems. Stable isotopes in ecological research. New York, NY: Springer; 1989. pp. 491–512.

87. Flockhart DTT, Kyser TK, Chipley D, Miller NG, Norris DR. Experimental evidence shows no fractionation of strontium isotopes (^{87}Sr/^{86}Sr) among soil, plants, and herbivores: Implications for tracking wildlife and forensic science. Isotopes Environ Health Stud. 2015; 51: 372–381. https://doi.org/10.1080/10256016.2015.1021345 PMID: 25789981

88. Beard B, Johnson C. Strontium isotope composition of skeletal material can determine the birth place and geographic mobility of humans and animals. J Forensic Sci. 2000; 45: 1049–1061. https://doi.org/10.1520/JFS14829J PMID: 11005180

89. Åberg G. The use of natural strontium isotopes as tracers in environmental studies. Water, Air, and Soil Pollution. 1995; 79: 309–322. https://doi.org/10.1007/BF01100444

90. Faure G, Mensing TM. Chapter 26: Hydrogen and oxygen. In: Faure G, Mensing TM, editors. Isotopes: Principles and Applications. New Jersey: John Wiley & Sons; 2005. pp. 693–752.

91. Hoefs J. Chapter 2: Isotope fractionation processes of selected elements. In: Hoefs J, editor. Stable Isotope Geochemistry. Cham, Switzerland: Springer International Publishing; 2015. pp. 76–88. https://doi.org/10.1007/978-3-319-19716-6

92. Longinelli A. Oxygen isotopes in mammal bone phosphate: A new tool for paleohydrological and paleo-climatological research? Geochim Cosmochim Acta. 1984; 48: 385–390. https://doi.org/10.1016/0016-7037(84)90259-X

93. Luz B, Kolodny Y, Horowitz M. Fractionation of oxygen isotopes between mammalian bone-phosphate and environmental drinking water. Geochim Cosmochim Acta. 1984; 48: 1689–1693. https://doi.org/10.1016/0016-7037(84)90338-7

94. Chenery CA, Pashley V, Lamb AL, Sloane HJ, Evans JA. The oxygen isotope relationship between the phosphate and structural carbonate fractions of human bioapatite: Relationship between phosphate and structural carbonate $\delta^{18}O$ in human enamel. Rapid Commun Mass Spectrom. 2012; 26: 309–319. https://doi.org/10.1002/rcm.5331 PMID: 22223318

95. Hermes T, Pederzani S, Makarewicz CA. Ahead of the curve? Implications for isolating vertical trans-humance in seasonal montane environments using sequential oxygen isotope analyses of tooth enamel. In: Ventresca Miller A, Makarewicz C, editors. Isotopic Investigations of Pastoralism in Prehistory. London and New York: Routledge; 2018. pp. 57–76.

96. Fricke HC, Clyde WC, O'Neil JR. Intra-tooth variations in $\delta^{18}O$ (PO_4) of mammalian tooth enamel as a record of seasonal variations in continental climate variables. Geochim Cosmochim Acta. 1998; 62: 1839–1850. https://doi.org/10.1016/S0016-7037(98)00114-8

97. Gigleux C, Grimes V, Tütken T, Knecht R, Britton K. Reconstructing caribou seasonal biogeography in Little Ice Age (late Holocene) Western Alaska using intra-tooth strontium and oxygen isotope analysis. J Archaeol Sci Rep. 2019; 23: 1043–1054. https://doi.org/10.1016/j.jasrep.2017.10.043

98. Faure G, Mensing TM. Chapter 27: Carbon. In: Faure G, Mensing TM, editors. Isotopes: Principles and Applications. New Jersey: John Wiley & Sons; 2005. pp. 753–802.

99. O'Leary H. Carbon isotope fractionation in plants. Phytochemistry. 1981; 20: 553–567. https://doi.org/10.1016/0031-9422(81)85134-5

100. Still CJ, Berry JA, Collatz GJ, DeFries RS. Global distribution of C_3 and C_4 vegetation: Carbon cycle implications. Glob Biogeochem Cycles. 2003; 17: 1006. https://doi.org/10.1029/2001GB001807

101. Balasse M. Reconstructing dietary and environmental history from enamel isotopic analysis: Time resolution of intra-tooth sequential sampling. Int J Osteoarchaeol. 2002; 12: 155–165. https://doi.org/10.1002/oa.601

102. Farquhar GD, Ehleringer JR, Hubick KT. Carbon isotope discrimination and photosynthesis. Annu Rev Plant Biol. 1989; 40: 503–537. https://doi.org/10.1146/annurev.pp.40.060189.002443

103. van der Merwe NJ, Medina E. The canopy effect, carbon isotope ratios and foodwebs in Amazonia. J Archaeol Sci. 1991; 18: 249–259. https://doi.org/10.1016/0305-4403(91)90064-V

104. Bocherens H, Drucker DG. Terrestrial teeth and bones. In: Elias SA, editor. Encyclopedia of Quaternary Science. Elsevier; 2007. pp. 309–317. https://doi.org/10.1016/B0-444-52747-8/00353-7

105. Chase B, Meiggs D, Ajithprasad P, Slater PA. Pastoral land-use of the Indus Civilization in Gujarat: Faunal analyses and biogenic isotopes at Bagasra. J Archaeol Sci. 2014; 50: 1–15. https://doi.org/10.1016/j.jas.2014.06.013

106. Ventresca Miller AR, Haruda A, Varfolomeev V, Goryachev A, Makarewicz CA. Close management of sheep in ancient Central Asia: Evidence for foddering, transhumance, and extended lambing seasons during the Bronze and Iron Ages. STAR Sci Technol Archaeol Res. 2020; 6: 41–60. https://doi.org/10.1080/20548923.2020.1759316

107. Lahtinen R. Main geological features of Fennoscandia. Geol Surv Finl Spec Pap. 2012; 53: 13–18.

108. Bergman S, Weihed P. Chapter 3 Archean (> 2.6 Ga) and Paleoproterozoic (2.5–1.8 Ga), pre-and syn-orogenic magmatism, sedimentation and mineralization in the Norrbotten and Överkalix lithotectonic units, Svecokarelian orogen. Geol Soc Lond Mem. 2020; 50: 27–82. https://doi.org/10.1144/M50-2016-29

109. Högdahl K, Bergman S. Chapter 5 Paleoproterozoic (1.9–1.8 Ga), syn-orogenic magmatism and sedimentation in the Ljusdal lithotectonic unit, Svecokarelian orogen. Geol Soc Lond Mem. 2020; 50: 131–153. https://doi.org/10.1144/M50-2016-30

110. Gee DG, Stephens MB. Chapter 19 Regional context and tectonostratigraphic framework of the early–middle Paleozoic Caledonide orogen, northwestern Sweden. Geol Soc Lond Mem. 2020; 50: 481–494. https://doi.org/10.1144/M50-2017-21

111. Gee DG, Klonowska I, Andréasson PG, Stephens MB. Chapter 21 Middle thrust sheets in the Caledonide orogen, Sweden: The outer margin of Baltica, the continent–ocean transition zone and late Cambrian–Ordovician subduction–accretion. Geol Soc Lond Mem. 2020; 50: 517–548. https://doi.org/10.1144/M50-2018-73

112. Erlström M. Chapter 24 Carboniferous–Neogene tectonic evolution of the Fennoscandian transition zone, southern Sweden. Geol Soc Lond Mem. 2020; 50: 603–620. https://doi.org/10.1144/M50-2016-25

113. Russell MJ, Smythe DK. Origin of the Oslo Graben in relation to the Hercynian-Alleghenian orogeny and lithospheric rifting in the North Atlantic. Tectonophysics. 1983; 94: 457–472. https://doi.org/10.1016/B978-0-444-42198-2.50031–6

114. Pawlewicz MJ, Williams AJ, Walden SM, Steinshouer DW. Generalized Geology of Europe including Turkey (geo4_2l): U.S. Geological Survey data release. 2003. Available: https://doi.org/10.5066/P9C8ZY5Q

115. Koch PL, Tuross N, Fogel ML. The effects of sample treatment and diagenesis on the isotopic integrity of carbonate in biogenic hydroxylapatite. J Archaeol Sci. 1997; 24: 417–429. https://doi.org/10.1006/jasc.1996.0126

116. Snoeck C, Pellegrini M. Comparing bioapatite carbonate pre-treatments for isotopic measurements: Part 1—Impact on structure and chemical composition. Chem Geol. 2015; 417: 394–403.

117. Martin C, Bentaleb I, Kaandorp R, Iacumin P, Chatri K. Intra-tooth study of modern rhinoceros enamel $\delta^{18}O$: Is the difference between phosphate and carbonate $\delta^{18}O$ a sound diagenetic test? Palaeogeogr Palaeoclimatol Palaeoecol. 2008; 266: 183–189. https://doi.org/10.1016/j.palaeo.2008.03.039

118. D'Angela D, Longinelli A. Oxygen isotopes in living mammal's bone phosphate: Further results. Chem Geol Isot Geosci Sect. 1990; 86: 75–82. https://doi.org/10.1016/0168-9622(90)90007-Y

119. Long ES, Sweitzer RA, Diefenbach DR, Ben-David M. Controlling for anthropogenically induced atmospheric variation in stable carbon isotope studies. Oecologia. 2005; 146: 148–156. https://doi.org/10.1007/s00442-005-0181-6 PMID: 16082561

120. Francey RJ, Allison CE, Etheridge DM, Trudinger CM, Enting IG, Leuenberger M, et al. A 1000-year high precision record of $\delta^{13}C$ in atmospheric $\delta^{18}O$. Tellus B. 1999; 51: 170–193. https://doi.org/10.1034/j.1600-0889.1999.t01-1-00005.x

121. Horwitz EP, Chiarizia R, Dietz ML. A novel strontium-selective extraction chromatographic resin. Solvent Extr Ion Exch. 1992; 10: 313–336. https://doi.org/10.1080/07366299208918107

122. Argentino C, Lugli F, Cipriani A, Panieri G. Testing miniaturized extraction chromatography protocols for combined $^{87}Sr/^{86}Sr$ and $\delta^{88/86}Sr$ analyses of pore water by MC-ICP-MS. Limnol Oceanogr Methods. 2021; 19: 431–440. https://doi.org/10.1002/lom3.10435

123. Lugli F, Cipriani A, Arnaud J, Arzarello M, Peretto C, Benazzi S. Suspected limited mobility of a Middle Pleistocene woman from Southern Italy: Strontium isotopes of a human deciduous tooth. Sci Rep. 2017; 7: 8615. https://doi.org/10.1038/s41598-017-09007-5 PMID: 28819227

124. Berglund M, Wieser ME. Isotopic compositions of the elements 2009 (IUPAC Technical Report). Pure Appl Chem. 2011; 83: 397–410. https://doi.org/10.1351/PAC-REP-10-06-02

125. Grimstead DN, Nugent S, Whipple J. Why a standardization of strontium isotope baseline environmental data is needed and recommendations for methodology. Adv Archaeol Pract. 2017; 5: 184–195. https://doi.org/10.1017/aap.2017.6

126. Britton K, Le Corre M, Willmes M, Moffat I, Grün R, Mannino MA, et al. Sampling plants and malacofauna in ($^{87}Sr/^{86}Sr$) bioavailability studies: Implications for isoscape mapping and reconstructing of past mobility patterns. Front Ecol Evol. 2020; 8: 579473. https://doi.org/10.3389/fevo.2020.579473

127. Holt E, Evans JA, Madgwick R. Strontium ($^{87}Sr/^{86}Sr$) mapping: A critical review of methods and approaches. Earth-Sci Rev. 2021; 216: 103593. https://doi.org/10.1016/j.earscirev.2021.103593

128. Hoogewerff JA, Reimann C, Ueckermann H, Frei R, Frei KM, van Aswegen T, et al. Bioavailable $^{87}Sr/^{86}Sr$ in European soils: A baseline for provenancing studies. Sci Total Environ. 2019; 672: 1033–1044. https://doi.org/10.1016/j.scitotenv.2019.03.387 PMID: 30999220

129. Bentley RA, Price TD, Stephan E. Determining the 'local' $^{87}Sr/^{86}Sr$ range for archaeological skeletons: A case study from Neolithic Europe. J Archaeol Sci. 2004; 31: 365–375. https://doi.org/10.1016/j.jas.2003.09.003

130. Liaw A, Wiener M. Classification and regression by randomForest. R News. 2002; 2: 18–22.

131. Gigante M, Mazzariol A, Bonetto J, Armaroli E, Cipriani A, Lugli F. Machine learning-based Sr isoscape of southern Sardinia: A tool for bio-geographic studies at the Phoenician-Punic site of Nora. Gimatzidis S, editor. PLoS ONE. 2023; 18: e0287787. https://doi.org/10.1371/journal.pone.0287787 PMID: 37467179

132. Genuer R, Poggi J-M, Tuleau-Malot C. VSURF: An R package for variable selection using random forests. R J. 2015; 7: 19–33. https://doi.org/10.32614/RJ-2015-018

133. Wright MN, Ziegler A. ranger: A fast implementation of random forests for high dimensional data in C++ and R. J Stat Softw. 2017; 77: 1–17. https://doi.org/10.18637/jss.v077.i01

134. Funck J, Bataille C, Rasic J, Wooller M. A bio-available strontium isoscape for eastern Beringia: A tool for tracking landscape use of Pleistocene megafauna. J Quat Sci. 2021; 36: 76–90. https://doi.org/10.1002/jqs.3262

135. Terzer S, Wassenaar LI, Araguás-Araguás LJ, Aggarwal PK. Global isoscapes for $\delta^{18}O$ and δ2H in precipitation: Improved prediction using regionalized climatic regression models. Hydrol Earth Syst Sci. 2013; 17: 4713–4728. https://doi.org/10.5194/hess-17-4713-2013

136. Laffoon JE, Sonnemann TF, Shafie T, Hofman CL, Brandes U, Davies GR. Investigating human geographic origins using dual-isotope ($^{87}Sr/^{86}Sr$, $\delta^{18}O$) assignment approaches. PLOS ONE. 2017; 12: e0172562. https://doi.org/10.1371/journal.pone.0172562 PMID: 28222163

137. Bataille CP, Jaouen K, Milano S, Trost M, Steinbrenner S, Crubézy É, et al. Triple sulfur-oxygen-strontium isotopes probabilistic geographic assignment of archaeological remains using a novel sulfur isoscape of western Europe. PLOS ONE. 2021; 16: e0250383. https://doi.org/10.1371/journal.pone.0250383 PMID: 33951062

138. Ma C, Vander Zanden HB, Wunder MB, Bowen GJ. assignR: An r package for isotope-based geographic assignment. Methods Ecol Evol. 2020; 11: 996–1001. https://doi.org/10.1111/2041-210X.13426

139. Zanon M, Davis BAS, Marquer L, Brewer S, Kaplan JO. European forest cover during the past 12,000 years: A palynological reconstruction based on modern analogs and remote sensing. Front Plant Sci. 2018; 9: 253. https://doi.org/10.3389/fpls.2018.00253 PMID: 29568303

140. Price JS, Allen S, Faucheux C, Althnaian T, Mount JG. Deer antlers: A zoological curiosity or the key to understanding organ regeneration in mammals? J Anat. 2005; 207: 603–618. https://doi.org/10.1111/j.1469-7580.2005.00478.x PMID: 16313394

141. Collins RP, Jones MB. The influence of climatic factors on the distribution of C_4 species in Europe. Vegetatio. 1986; 64: 121–129. https://doi.org/10.1007/BF00044788

142. Bataille CP, Brennan SR, Hartmann J, Moosdorf N, Wooller MJ, Bowen GJ. A geostatistical framework for predicting variations in strontium concentrations and isotope ratios in Alaskan rivers. Chem Geol. 2014; 389: 1–15. https://doi.org/10.1016/j.chemgeo.2014.08.030

143. Johnson L, Evans J, Montgomery J, Chenery C. The forest effect: Biosphere $^{87}Sr/^{86}Sr$ shifts due to changing land use and the implications for migration studies. Sci Total Environ. 2022; 839: 156083. https://doi.org/10.1016/j.scitotenv.2022.156083 PMID: 35598659

144. Goss RJ. The diversity of deer. Deer antlers: Regeneration, function and evolution. New York, USA: Academic Press; 1983. pp. 31–32.

145. Lachniet MS, Lawson DE, Stephen H, Sloat AR, Patterson WP. Isoscapes of $\delta^{18}O$ and δ^2H reveal climatic forcings on Alaska and Yukon precipitation: Alaska isoscape. Water Resour Res. 2016; 52: 6575–6586. https://doi.org/10.1002/2016WR019436

146. Janzen A, Bataille C, Copeland SR, Quinn RL, Ambrose SH, Reed D, et al. Spatial variation in bioavailable strontium isotope ratios ($^{87}Sr/^{86}Sr$) in Kenya and northern Tanzania: Implications for ecology, paleoanthropology, and archaeology. Palaeogeogr Palaeoclimatol Palaeoecol. 2020; 560: 109957. https://doi.org/10.1016/j.palaeo.2020.109957

147. Wang X, Tang Z. The first large-scale bioavailable Sr isotope map of China and its implication for provenance studies. Earth-Sci Rev. 2020; 210: 103353. https://doi.org/10.1016/j.earscirev.2020.103353

148. St John Glew K, Espinasse B, Hunt BPV, Pakhomov EA, Bury SJ, Pinkerton M, et al. Isoscape models of the Southern Ocean: Predicting spatial and temporal variability in carbon and nitrogen isotope compositions of particulate organic matter. Glob Biogeochem Cycles. 2021; 35: e2020GB006901. https://doi.org/10.1029/2020GB006901

149. Lugli F, Cipriani A, Bruno L, Ronchetti F, Cavazzuti C, Benazzi S. A strontium isoscape of Italy for provenance studies. Chem Geol. 2022; 587: 120624. https://doi.org/10.1016/j.chemgeo.2021.120624

150. Hundertmark KJ. Home range, dispersal and migration. In: Franzmann AW, Schwartz CC, editors. Ecology and management of the North American moose Smithsonian Institution Press. Washington, DC, USA: Smithsonian Institution Press; 1998. pp. 303–335.

151. Seiler A, Cederlund G, Jernelid H, Grängstedt P, Ringaby E. The barrier effect of highway E4 on migratory moose (*Alces alces*) in the High Coast area, Sweden. In: Turcott E, editor. Proceedings of the IENE International Conference on "Habitat fragmentation due to transport infrastructure." Brussells, Belgium; 2003. pp. 1–18.

152. Riofrío-Lazo M, Aurioles-Gamboa D. Timing of isotopic integration in marine mammal skull: Comparative study between calcified tissues. Rapid Commun Mass Spectrom. 2013; 27: 1076–1082. https://doi.org/10.1002/rcm.6556 PMID: 23592211

153. Fahy GE, Deter C, Pitfield R, Miszkiewicz JJ, Mahoney P. Bone deep: Variation in stable isotope ratios and histomorphometric measurements of bone remodelling within adult humans. J Archaeol Sci. 2017; 87: 10–16. https://doi.org/10.1016/j.jas.2017.09.009

154. Eriksen A, Wabakken P, Zimmermann B, Andreassen HP, Arnemo JM, Gundersen H, et al. Encounter frequencies between GPS-collared wolves (*Canis lupus*) and moose (*Alces alces*) in a Scandinavian wolf territory. Ecol Res. 2009; 24: 547–557. https://doi.org/10.1007/s11284-008-0525-x

155. Olsson M, Cox JJ, Larkin JL, Widén P, Olovsson A. Space and habitat use of moose in southwestern Sweden. Eur J Wildl Res. 2011; 57: 241–249. https://doi.org/10.1007/s10344-010-0418-5

156. Hauge TM, Keith LB. Dynamics of moose populations in northeastern Alberta. J Wildl Manag. 1981; 45: 573–597. https://doi.org/10.2307/3808692

157. Doerr JG. Home range size, movements and habitat use in two moose, *Alces alces*, populations in southeastern Alaska. Can Field-Nat. 1983; 97: 79–88.

158. Timmermann HR, McNicol JG. Moose habitat needs. For Chron. 1988; 64: 238–245. https://doi.org/10.5558/tfc64238-3

159. Leptich DJ, Gilbert JR. Summer home range and habitat use by moose in northern Maine. J Wildl Manag. 1989; 53: 880–885. https://doi.org/10.2307/3809581

160. Van Dyke F, Probert BL, Van Beek GM. Moose home range fidelity and core area characteristics in south-central Montana. Alces J Devoted Biol Manag Moose. 1995; 31: 93–104.

161. Oehlers SA, Bowyer RT, Huettmann F, Person DK, Kessler WB. Sex and scale: Implications for habitat selection by Alaskan moose *Alces alces gigas*. Wildl Biol. 2011; 17: 67–84. https://doi.org/10.2981/10-039

162. Cederlund G, Sandegren F, Larsson K. Summer movements of female moose and dispersal of their offspring. J Wildl Manag. 1987; 51: 342–352. https://doi.org/10.2307/3801014

163. Sandegren F, Bergström R, Cederlund G, Dansie E. Spring migration of female moose in central Sweden. Alces J Devoted Biol Manag Moose. 1982; 18: 210–234.

164. Van Ballenberghe VV. Migratory behavior of moose in southcentral Alaska. Int Congr Game Biol. 1977; 13: 103–109.

165. Hoffman JD, Genoways HH, Choate JR. Long-distance dispersal and population trends of moose in the central United States. Alces J Devoted Biol Manag Moose. 2006; 42: 115–131.

166. Eriksson G, Frei KM, Howcroft R, Gummesson S, Molin F, Lidén K, et al. Diet and mobility among Mesolithic hunter-gatherers in Motala (Sweden) - The isotope perspective. J Archaeol Sci Rep. 2018; 17: 904–918. https://doi.org/10.1016/j.jasrep.2016.05.052

167. Evans JA, Tatham S. Defining 'local signature' in terms of Sr isotope composition using a tenth- to twelfth-century Anglo-Saxon population living on a Jurassic clay-carbonate terrain, Rutland, UK. Geol Soc Lond Spec Publ. 2004; 232: 237–248. https://doi.org/10.1144/GSL.SP.2004.232.01.21

168. Heaton THE. Spatial, species, and temporal variations in the ^{13}C/^{12}C ratios of C$_3$ plants: Implications for palaeodiet studies. J Archaeol Sci. 1999; 26: 637–649. https://doi.org/10.1006/jasc.1998.0381

169. Walter WD, Leslie DM. Stable isotope ratio analysis to differentiate temporal diets of a free-ranging herbivore: SIRA to differentiate temporal diets of free-ranging herbivores. Rapid Commun Mass Spectrom. 2009; 23: 2190–2194. https://doi.org/10.1002/rcm.4135 PMID: 19530151

170. Pyankov VI, Ziegler H, Akhani H, Deigele C, Lüttge U. European plants with C$_4$ photosynthesis: Geographical and taxonomic distribution and relations to climate parameters. Bot J Linn Soc. 2010; 163: 283–304. https://doi.org/10.1111/j.1095-8339.2010.01062.x

171. Osborne CP, Salomaa A, Kluyver TA, Visser V, Kellogg EA, Morrone O, et al. A global database of C4 photosynthesis in grasses. New Phytol. 2014; 204: 441–446. https://doi.org/10.1111/nph.12942 PMID: 25046685

172. Niedziałkowska M, Neumann W, Borowik T, Kołodziej-Sobocińska M, Malmsten J, Arnemo JM, et al. Moose *Alces alces* (Linnaeus, 1758). In: Corlatti L, Zachos FE, editors. Terrestrial Cetartiodactyla–Handbook of the mammals of Europe. Cham: Springer International Publishing; 2022. pp. 215–246. https://doi.org/10.1007/978-3-030-24475-0

173. Månsson J, Kalén C, Kjellander P, Andrén H, Smith H. Quantitative estimates of tree species selectivity by moose (*Alces alces*) in a forest landscape. Scand J For Res. 2007; 22: 407–414. https://doi.org/10.1080/02827580701515023

174. Loisa K, Pulliainen E. Winter food and movements of two moose (*Alces alces* L.) in northeastern Finland. Ann Zool Fenn. 1968; 5: 220–223.

175. Sæther B-E, Andersen R. Resource limitation in a generalist herbivore, the moose *Alces alces*: Ecological constraints on behavioural decisions. Can J Zool. 1990; 68: 993–999. https://doi.org/10.1139/z90-143

176. Wam HK, Hjeljord O. Moose summer and winter diets along a large scale gradient of forage availability in southern Norway. Eur J Wildl Res. 2010; 56: 745–755. https://doi.org/10.1007/s10344-010-0370-4

177. Berlioz E, Leduc C, Hofman-Kamińska E, Bignon-Lau O, Kowalczyk R, Merceron G. Dental microwear foraging ecology of a large browsing ruminant in Northern Hemisphere: The European moose (*Alces alces*). Palaeogeogr Palaeoclimatol Palaeoecol. 2022; 586: 110754. https://doi.org/10.1016/j.palaeo.2021.110754

178. Schwartz CC. Physiological and nutritional adaptations of moose to northern environments. Alces J Devoted Biol Manag Moose. 1992; 139–155.

179. Nikula A, Heikkinen S, Helle E. Habitat selection of adult moose Alces alces at two spatial scales in central Finland. Wildl Biol. 2004; 10: 121–135. https://doi.org/10.2981/wlb.2004.017

180. Bowling DR, Pataki DE, Randerson JT. Carbon isotopes in terrestrial ecosystem pools and CO_2 fluxes. New Phytol. 2008; 178: 24–40. https://doi.org/10.1111/j.1469-8137.2007.02342.x PMID: 18179603

181. Shipley LA, Blomquist S, Danell K. Diet choices made by free-ranging moose in northern Sweden in relation to plant distribution, chemistry, and morphology. Can J Zool. 1998; 76: 1722–1733. https://doi.org/10.1139/z98-110

182. Drucker DG, Bridault A, Hobson KA, Szuma E, Bocherens H. Can carbon-13 in large herbivores reflect the canopy effect in temperate and boreal ecosystems? Evidence from modern and ancient ungulates. Palaeogeogr Palaeoclimatol Palaeoecol. 2008; 266: 69–82. https://doi.org/10.1016/j.palaeo.2008.03.020

183. Melin M, Matala J, Mehtätalo L, Tiilikainen R, Tikkanen O-P, Maltamo M, et al. Moose (*Alces alces*) reacts to high summer temperatures by utilizing thermal shelters in boreal forests - an analysis based on airborne laser scanning of the canopy structure at moose locations. Glob Change Biol. 2014; 20: 1115–1125. https://doi.org/10.1111/gcb.12405 PMID: 24115403

184. van Beest FM, Van Moorter B, Milner JM. Temperature-mediated habitat use and selection by a heat-sensitive northern ungulate. Anim Behav. 2012; 84: 723–735. https://doi.org/10.1016/j.anbehav.2012.06.032

185. Trolier M, White JWC, Tans PP, Masarie KA, Gemery PA. Monitoring the isotopic composition of atmospheric CO_2: Measurements from the NOAA Global Air Sampling Network. J Geophys Res Atmospheres. 1996; 101: 25897–25916. https://doi.org/10.1029/96JD02363

186. Parker KL, Barboza PS, Stephenson TR. Protein conservation in female caribou (*Rangifer tarandus*): Effects of decreasing diet quality during winter. J Mammal. 2005; 86: 610–622. https://doi.org/10.1644/1545-1542(2005)86[610:PCIFCR]2.0.CO;2

187. Davis CL, Guralnick RP, Zipkin EF. Challenges and opportunities for using natural history collections to estimate insect population trends. J Anim Ecol. 2023; 92: 237–249. https://doi.org/10.1111/1365-2656.13763 PMID: 35716080